MEASUREMENT OF ROCKET NOZZLE SURFACE RECESSION USING SPECTROSCOPIC TECHNIQUES

Wendell A. Stephen and Thomas E. Frakes
United Technology Center

TECHNICAL REPORT AFRPL-TR-72-91
OCTOBER 1972
CONTRACT NO. F04611-71-C-0041

United States Air Force
Air Force Systems Command
Air Force Rocket Propulsion Laboratory (MKMC)
Edwards, California 93523

Details of illustrations in this document may be better studied on microfiche

DISCLAIMER NOTICE

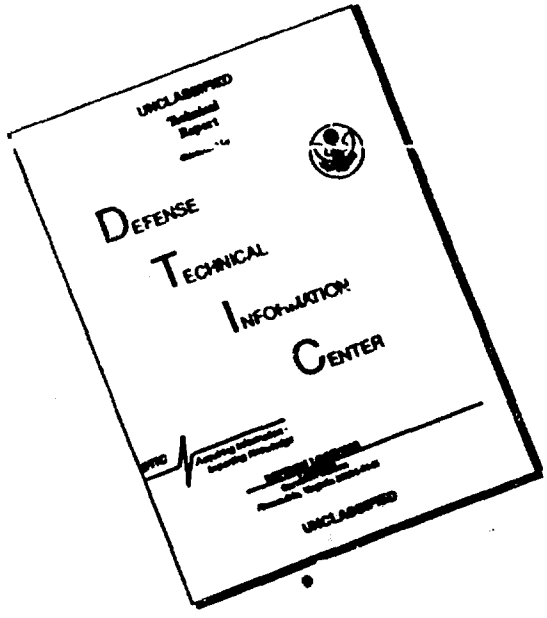

THIS DOCUMENT IS BEST QUALITY AVAILABLE. THE COPY FURNISHED TO DTIC CONTAINED A SIGNIFICANT NUMBER OF PAGES WHICH DO NOT REPRODUCE LEGIBLY.

Unclassified
Security Classification

DOCUMENT CONTROL DATA – R & D

(Security classification of title, body of abstract and indexing annotation must be entered when the overall report is classified)

1. ORIGINATING ACTIVITY *(Corporate author)*
United Technology Center
Division of United Aircraft Corporation
Sunnyvale, California

2a. REPORT SECURITY CLASSIFICATION
Unclassified

2b. GROUP

3. REPORT TITLE
Measurement of Rocket Nozzle Surface Recession Using Spectrographic Techniques

4. DESCRIPTIVE NOTES *(Type of report and inclusive dates)*
Final Report

5. AUTHOR(S) *(First name, middle initial, last name)*
Wendell A. Stephen and Thomas E. Frakes

6. REPORT DATE	7a. TOTAL NO. OF PAGES	7b. NO. OF REFS
October 1972	65	0

8a. CONTRACT OR GRANT NO.	9a. ORIGINATOR'S REPORT NUMBER(S)
F04611-71-C-0041	UTC 2405-FR
b. PROJECT NO. UTC 2405-FR	
c.	9b. OTHER REPORT NO(S) *(Any other numbers that may be assigned this report)* AFRPL-TR-72-91
d.	

10. DISTRIBUTION STATEMENT
Approved for public release; distribution unlimited

11. SUPPLEMENTARY NOTES	12. SPONSORING MILITARY ACTIVITY
	United States Air Force Air Force Systems Command Air Force Rocket Propulsion Laboratory (MKNC) Edwards, California

13. ABSTRACT

The objective of this program was to design, analyze, and evaluate experimentally the surface recession of ablative materials using spectrographic techniques. This program was accomplished in two phases. The first phase was the design, analysis, and development of a containment system for the tracer elements. The second phase was the demonstration of the feasibility of that system during static firings in two rocket nozzles, one fabricated from carbon-phenolic and the other from silica-phenolic with a codeposited silicon carbide/pyrolytic-graphite throat insert. Laboratory tests were conducted with a plasma-arc torch to verify the capsule design. The capsules, with thermocouples, were then tested in a solid rocket motor at a pressure of 800 psi with 16%-aluminized polybutadiene-acrylic acid-acrylonitrile propellant. The test results showed poor correlation between the ablation as indicated by thermocouples and that indicated by detection of the tracer salts. This report describes the various program activities from initial tracer selection and configuration selection to final test firing demonstration and analysis of test results.

DD FORM 1 NOV 65 1473

Unclassified
Security Classification

14. KEY WORDS	LINK A		LINK B		LINK C	
	ROLE	WT	ROLE	WT	ROLE	WT
nozzle ablation						
spectrographic technique						

MEASUREMENT OF ROCKET NOZZLE SURFACE RECESSION USING SPECTROSCOPIC TECHNIQUES

Wendell A. Stephen
and
Thomas E. Frakes

UTC 2405-FR

FOREWORD

This technical report summarizes work performed from 15 March 1971 to 31 July 1972 under Contract No. F04611-71-C-0041 by United Technology Center, Sunnyvale, California, for Air Force Rocket Propulsion Laboratory, Edwards, California. This contract results from United Technology Proposal No. 70-67, "Measurement of Rocket Nozzle Surface Recession Using Spectrographic Techniques," issued in response to Air Force request for quotation No. F04611-71-Q-0017.

The work reported herein was performed under the technical direction of Capt. W. Lewandowski of the Air Force Rocket Propulsion Laboratory. The United Technology Center program manager was Mr. W. A. Stephen, and the project engineer was Mr. T. E. Frakes.

Special recognition should be given to Mr. M. E. Nelson, Mr. O. Sihner, Dr. J. C. Trowbridge, and Mr. P. G. Willoughby for their technical contribution.

This technical report has been reviewed and is approved.

Jerry N. Mason
Captain, U.S. Air Force

ABSTRACT

The objective of this program was to design, analyze, and evaluate experimentally the surface recession of ablative materials using spectrographic techniques. This program was accomplished in two phases. The first phase was the design, analysis, and development of a containment system for the tracer elements. The second phase was the demonstration of the feasibility of that system during static firings in two rocket nozzles, one fabricated from carbon-phenolic and the other from silica-phenolic with a codeposited silicon carbide/pyrolytic-graphite throat insert. Laboratory tests were conducted with a plasma-arc torch to verify the capsule design. The capsules, with thermocouples, were then tested in a solid rocket motor at a pressure of 800 psi with 16%-aluminized polybutadiene-acrylic acid-acrylonitrile propellant. The test results showed poor correlation between the ablation as indicated by thermocouples and that indicated by detection of the tracer salts. This report describes the various program activites from initial tracer selection and configuration selection to final test firing demonstration and analysis of test results.

CONTENTS

ILLUSTRATIONS

ILLUSTRATIONS (Continued)

TABLES

SECTION I

INTRODUCTION

Advancements in the solid rocket industry in high flame temperature propellants, elevated chamber pressure, increased duration, and multicycle operation require the evaluation of compatible ablative type materials. These materials must possess low ablation and thermal penetration characteristics. The ablation characteristics of the materials may be predicted analytically or evaluated during test firings. Normally, ablation results from test firings are limited to only the posttest measurement and do not give a chronological record to check the accuracy of the analytical technique during the firing. This chronological recording is especially important in a location where the flow field is not well defined and changes drastically throughout the firing, such as in the region of a slotted propellant grain.

Limited attempts have been made, with varying degrees of success, to measure the ablation rate in-situ during rocket firings. Techniques such as insertion of probes (thermocouples, breakwires, etc.) and ablative needles using radioactive isotopes have been used. The insertion of probes requires electrical leads to be brought through the highly stressed combustion chamber. The radioactive needle requires sophisticated handling and recording procedures. It also is quite expensive for small material evaluation programs.

UTC has used passive inert tracers embedded in solid propellant to define the burnback characteristics by detecting their arrival in the plume using spectroscopic measurements. This method is simple and inexpensive, is readily available, and the recording instrumentation may be located some distance from the test stand.

Since this technique has proven to be highly successful in the definition of propellant receding surfaces during motor operation, it was proposed that the same method be applied to the ablating hotside nozzle materials. This is considerably more challenging since considerable thermal penetration is encountered on the hotside nozzle material, resulting in temperatures in the component that are sufficiently high to vaporize the salt tracers prior to the time the salt region is exposed. Therefore, the salts have to be thermally protected or contained until the region where the salts are contained is exposed to the flame front.

SECTION II

SUMMARY

This report summarizes the work conducted by UTC under AFRPL Contract No. F04611-71-C-0041. A two-phase technical program was conducted with the primary objective of designing, analyzing, and evaluating experimentally the surface recession of ablative nozzle materials by using metallic salt tracers which are detected in the exhaust plume by spectrographic techniques.

The expected accomplishments were to demonstrate the dynamic measurement of ablative material response in a solid rocket environment within ±10% of that defined by in-depth thermocouple measurements.

Metallic tracer salts were contained in insulated capsules using Union Carbide Grafoil as the thermal barrier. This concept was demonstrated in the laboratory using actual tracer salts and capsules embedded in a block of carbon-phenolic which was subjected to a high heat flux environment. This resulted in both thermal penetration and material removal.

The encapsulation technique was then incorporated into two test nozzles which were test fired on a solid rocket motor at AFRPL. The test results showed that the technique was so erratic and unreliable that the expected accomplishments were not attained.

The two program phase activities are summarized in the following two subsections.

1. PHASE I - INSTRUMENTATION DESIGN

The design of the encapsulation method was based on both thermal penetration analysis and selection of capsule materials and tracer salts. The thermal analysis involved defining the in-depth gradient for various candidate capsule materials. These analyses were one-dimensional models since the effects of charring were of paramount importance and the two-dimensional models do not account for this effect.

The tracer salts to be evaluated were selected based on previous test firing experience at UTC where the detection of their presence in the exhaust plume has been demonstrated successfully. The compounds of rubidium, lithium, and cesium were chosen for test evaluation.

Laboratory tests were conducted on candidate capsule materials to define performance when embedded in a charring phenolic ablator. All materials evaluated were completely charred considerably earlier than the predicted time of exposure. These materials became a porous ash without structural adequacy and were therefore unacceptable. Prechar materials were then evaluated and Union Carbide Grafoil was selected based on the structural integrity, reduced thermal conductivity, and availability.

Laboratory tests were conducted using actual tracer salts contained in Grafoil capsules which were embedded in blocks of graphite-phenolic. In-depth thermocouple instrumentation was used to verify the time of exposure. The specimens were subjected to a high flux environment generated by a plasma-arc torch. The torch was oriented at 45° to the specimen surface to result in both a high thermal penetration plus ablation of the specimen material. Spectographic cameras were used to detect the time of tracer salt release. Based on these tests the time of tracer release correlated within 68 msec of the time the surface receded to the capsule location.

2. PHASE II - NOZZLE DESIGN, EVALUATION, AND POSTTEST ANALYSIS

Based on the successful results during the laboratory program, this tracer encapsulation technique was incorporated into nozzle designs using both carbon- and silica-phenolic. The designs were monolithic flat laminate molding of Fiberite Corp. MX4926 carbon-phenolic and MX2600 silica-phenolic machined to the desired internal contour for a 2.3-in.-diameter throat. The silica-phenolic design incorporated a GFE codeposited silicon carbide/pyrolytic-graphite-coated throat insert since the ablation rate of silica-phenolic would be excessive, resulting in low motor operating pressures.

Two salt capsules were located at various depths in each of a subsonic and supersonic location for both nozzles. A thermocouple plug was installed in between the two plugs at each location to provide thermal gradients during firing for evaluation of the instrumentation accuracy. Thermocouples were also installed in the capsules to verify the time of exposure to the flame.

The nozzles were tested at AFRPL on the 36-in. CHAR motor using a cured solid propellant end burning grain with UTP-3001b (84% solids-loaded PBAN with 16% aluminum content). Only three of the eight tracer capsules were exposed during the two firings due to lower ablation than predicted. These three tracers were detected in the exhaust plume by a spectographic technique. The results of the test firings reveal that the time of ejection of the tracers into the exhaust stream is inconsistent for the configuration used. Two of the three tracers were injected early whereas the third performed as predicted.

Posttest sectioning of the nozzle ablatives revealed that two of the capsules remained intact and were essentially ready to be exposed at firing shutdown. This fact demonstrates the salts were being contained in those individual capsules; however, the technique appears to be unreliable as shown by the early ejection on the other two units mentioned previously.

It is not recommended to continue the activities further unless considerable funding may be allocated to allow considerable effort to be expended in developing a suitable thermal protection capsule.

SECTION III

CONTRACT OBJECTIVES

The program objectives were to design, analyze, and evaluate experimentally the surface recession of ablative nozzle materials using spectrographic detection techniques.

SECTION IV

EXPECTED ACCOMPLISHMENTS

The expected accomplishments of this program were to:

A. Define the instrumentation design which will measure in-situ ablation depth at discrete points.

B. Define the containment method for the tracer which will not affect the carbon and silica-phenolic surface temperature to the extent that the ablation rate will be altered by more than ±10%.

C. Verify by laboratory plasma-arc testing that the thermal penetration and tracer exposure criteria established by heat transfer analysis is met for the proposed design.

D. Demonstrate during full-scale static firings that ablative insulator surface recession can be measured within ±10% using spectrographic techniques when compared to recorded thermocouple data.

SECTION V

PHASE I - INSTRUMENTATION DESIGN

1. TRACER SELECTION

The selection of individual metallic salt tracers was based primarily on experience gained from past UTC motor firings. Analyses of the spectrum of a rocket plume has shown that it is composed of continuum radiation from the liquid and solid particles present and of atomic lines and molecular bands due to atomic and molecular species in the hot gas. A suitable tracer must be an element not already in large concentration, must give an intense line likely to be detectable above the continuum radiation, and must have lines or bands at a wavelength for which a detector of high sensitivity is available. In general, the wavelength region between 0.3 and 0.9 micron is the most suitable. Sensitive photomultiplier detectors are available for this region, and the continuum radiation, even with aluminum present in the gas stream, is low enough relative to black-body radiation to let individual lines and bands stand out clearly. Also, there is not significant atmospheric absorption to interfere with observation at distances up to a mile.

Candidate tracers, along with the line wavelengths and the relative quantities of salts required to produce equal spectral response, are presented in table I. All of these candidates possess satisfactory wavelengths. The required relative quantities of strontium, barium, radium, and calcium are considerably more than the other tracers, indicating these elements are less desirable. The required salt addition rate into the exhaust stream was determined theoretically from an analysis of the optical radiation from the rocket plume as presented in the appendix. The analysis is based on sodium chloride with the relative quantities for each of the other tracers calculated by properly accounting for their optical properties and the molecular weight.

The sodium chloride data presented in figure 1 are for a filter transmission band width of 2.0, which is characteristic of the detection instrumentation used on this project. This curve has been verified by making spectral measurements on the plumes of solid rocket motors ranging in size from the UTC 4-lb test motor to a full-scale, seven-segment, 120-in.-diameter motor. The actual amount of salt that must be inserted at each point depends upon the time needed to observe and record the signal. Previous experience has shown that approximately 100 msec is sufficient to obtain tracer detection in the exhaust. The capsules contained more than the required quantity of tracer material to ensure the detection in the exhaust stream.

Tracers containing lithium, cesium, rubidium, sodium, potassium, barium, indium, strontium, and calcium have been evaluated on actual rocket static test firings at UTC. Satisfactory results have been obtained with lithium, cesium, and rubidium using the UTC-formulated PBAN propellants. It was shown in these tests that sodium and potassium lines are present in the propellant exhaust of the basic UTC PBAN propellant. Therefore, these elements are not acceptable for tracer detection. The lines of barium, indium, strontium, and calcium did not

TABLE I

THEORETICAL RELATIVE QUANTITIES OF SALTS REQUIRED
TO PRODUCE EQUAL SPECTRAL RADIANCE

Salt	Line Wavelength micron	Relative Mass Required
Sodium chloride	0.5890	1.00
Potassium chloride	0.7665	0.14
Lithium fluoride	0.6708	0.19
Rubidium sulfate	0.7800	0.12
Cesium sulfate	0.8521	0.21
Strontium fluoride	0.4607	79.00
Indium	0.4511	37.00
Barium fluoride	0.5535	5.20
Calcium fluoride	0.4227	138.00

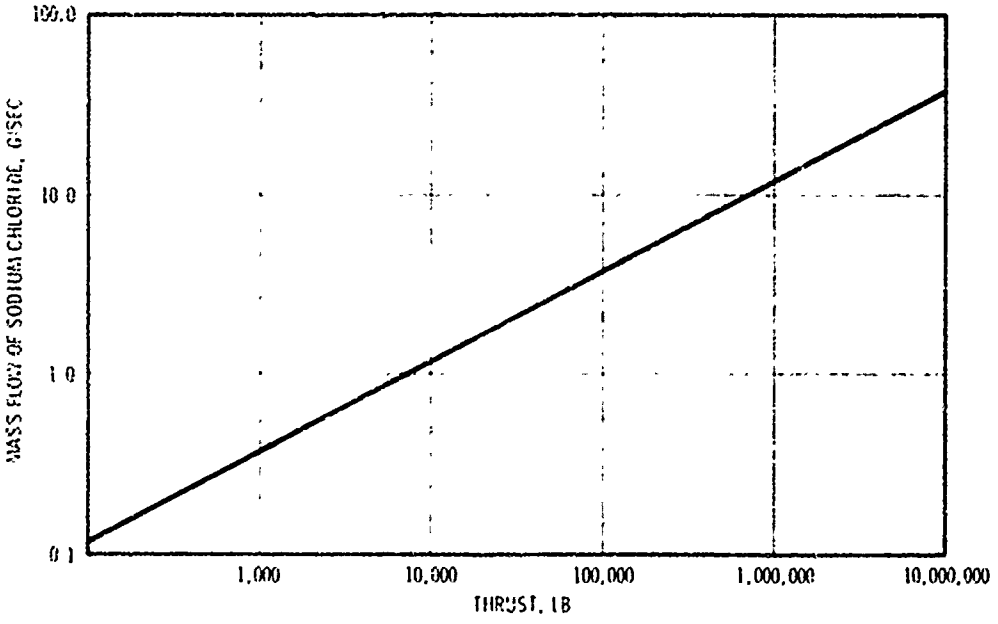

Figure 1. Correlation Curve for Mass Flow of Sodium Chloride Required for Detection by Spectrograph in the Exhaust of Rocket Motors

show above the continuum when using masses comparable to the other tracers. This result confirms the theoretical results (table I) that the quantity of these tracers has to be much higher to be detectable.

Boiling point and required volume of solid-state material were selection considerations in addition to detectability. For installations where the tracer element is contained in a solid state up to the time of exposure, a high melting temperature (which requires less thermal protection) and low volume (which has less effect on phenolic surface temperature) is required. Table II presents the solid-state mass and volume requirements for the three tracers. Lithium fluoride has a high boiling point (3,050°F) and also requires a low solid volume. Therefore, it was a prime candidate for use in the insulated solid-state capsule. Cesium sulfate also requires a low amount of solid volume to be detectable. Rubidium sulfate also was chosen as a candidate because it requires the least volume of gas necessary to obtain detectable spectral lines. This is due to both a reduction in the required solid-state mass and an increased molecular weight.

To increase the amount of data obtained from each test, a minimum of two capsules were placed at different depths for each area ratio location. The tracer elements used throughout the nozzles (both at different depths at one location and at different locations) were selected to provide discrete spectral response so that verification of the sequence of injection from each capsule could be detected easily.

TABLE II

REQUIRED QUANTITIES
OF THE CANDIDATE TRACER ELEMENTS

Tracer Compound	Mass, g*	Solid-State Volume, cm†
Rubidium sulfate	0.09	0.05
Lithium fluoride	0.14	0.11
Cesium sulfate	0.15	0.07

*Based on 1.0-sec injection.
†Based on 50% compaction.

2. CAPSULE MATERIAL SELECTION

The accuracy of the surface recession measurement using metallic tracers is dependent on the time the tracer enters the gas stream and its concentration at that time. Therefore, the method of installation may vary for various ablative insulators since a wide variation of the temperature penetration exists.

The one extreme is a high charring insulator of carbon-phenolic such as that used in nozzle S/N 01. A typical carbon-phenolic char layer may be approximately 0.35-in. thick, and the temperature line corresponding to the tracer boiling point (2,500° to 3,000°F) lies approximately 0.12 in. below the surface. To obtain the desired accuracy of ±10%, it is necessary to delay the time of injection of the tracer into the exhaust stream to more nearly correspond to the surface recession. Since the boiling point is reached considerably before the time of actual surface recession, the tracer has to be thermally protected.

The other extreme is a high ablating silica-phenolic such as that used in nozzle S/N 02. The resulting high ablation and silica melt runoff results in minimum thermal penetration. Therefore, the temperature line for the boiling point of the tracer is essentially at the surface. This allows the salts to be contained in a low melting point capsule. Once exposed, the salts will gasify immediately and enter the stream.

The most desirable method is to provide thermal protection for the salts so that the boiling point is reached coincidentally with the material surface receding to the depth of the tracer location. Once the salts start to vaporize, the protection capsule is fractured allowing the tracer to be injected into the gas stream. This system allows containment of the salts in a capsule that is just large enough to accommodate the required volume of the solid-state material and, therefore, provides minimal effect on the ablating surface due to a heat sink effect.

Even though the temperature is maintained sufficiently low to prevent salt vaporization, the possibility exists that the salts will start to sublime and leach up through the char layer in sufficient quantity to allow detection of the salts prematurely before the capsules are exposed.

An estimate of the rates of diffusion of salt vapors through a thin section of carbon-phenolic nozzle material was made using a relatively simple model. Because of the uncertainties in diffusivities, porosity, thermal gradients within the pellet, and pyrolysis product flow around the pellet, only order of magnitude accuracy was feasible for this simple analysis. The salts considered were rubidum sulfate, lithium fluoride, and cesium chloride.

The analysis showed that there was a potential for possible injection of the tracer elements into the exhaust stream 5 sec prior to that desired if the carbon-phenolic medium surrounding the salts had a porosity of 20% which is typical of the charred material. The diffusion of the salts through the porous layer is due to a sublimation process. Since the nozzle pressure at

the capsule locations increases the boiling point to approximately 4,390°F, the pressure gradient and resulting flow of the tracer element is sufficiently low so that a relatively weak impervious material may be used to contain the tracer.

The initial two materials considered were silicone rubber and zinc chromate putty. Thermal and diffusion analysis indicated that the presence of typical thicknesses for these materials would not significantly increase ablation rates of the surrounding phenolic.

Since the thermal conductivities of silicone rubber and zinc chromate putty were not defined above 600°F, laboratory tests were conducted. The laboratory evaluation tests showed that the silicone rubber and zinc chromate putty became a porous ash at temperatures above 1,000°F, which made them unsuitable for the capsule material. Since all materials will char at these temperatures, it was decided to evaluate prechars or graphitic base materials.

Union Carbide's Grafoil was selected because it remains impervious to gas flow at temperatures above the anticipated maximum capsule temperature (4,200°F), has relatively good insulative properties normal to the surface, is readily available, and may be fabricated easily into a capsule.

3. THERMAL ANALYSIS CAPSULE DESIGN SUPPORT

Thermal analyses were conducted to define the limiting cases of capsule wall thickness and their effect on the ablating surface temperature. Since these effects are paramount in the carbon-phenolic and may be ignored in the silica-phenolic, the evaluation was limited to the carbon-phenolic nozzle. The heat transfer mechanism is two-dimensional and should ideally be analyzed using an appropriate two-dimensional thermal model. However, the two-dimensional analysis model does not include the effects of charring. The effect of charring is of major significance in defining the thermal penetration through the nozzle materials. Therefore, all analyses were one-dimensional which should be conservative since the effect of axial heat transfer is ignored. All analyses were conducted for a constant pressure of 800 psia with a maximum duration of 30 sec using UTP-3001 propellant properties.

The initial analysis was made to define the worst case effect of the capsule on the ablating surface temperature. The model for this analysis assumed an initial thickness of 0.1-in. ablating carbon-phenolic covering an infinite thickness of the silicone rubber capsule material. The 0.1-in. carbon-phenolic represents half of the total predicted ablation depth at the selected instrumentation locations. This analysis was ultraconservative in that the capsule material was not allowed to char (i.e., room temperature thermal conductivities were used). A similar analysis was made for the parent phenolic with the capsule. These two analyses were then compared to define the maximum effect of the presence of the noncharring capsule. This conservative approach showed that the effect on surface temperature due to the silicone rubber capsule was 450°F. An equilibrium surface temperature analysis was conducted which demonstrated that the differential in surface temperature increased the total ablation at time of exposure by 10%. This analysis also showed that a 0.050-in. minimum thickness of silicone capsule rubber would be required to maintain the salts below 3,000°F, provided the rubber did not char.

An analysis was performed accounting for the change in the capsule material thermal conductivity versus temperature. Since the thermal conductivity for silicone rubber is not defined above 600°F, the high-temperature properties were estimated. It was assumed that the fully charred silicone rubber would have the same conductivity as the charred phenolic material. This assumption resulted in defining the maximum thickness of required capsule material since the fully charred silicone rubber would be more porous than the phenolic and, therefore, would have a lower thermal conductivity. Using a model with 0.1-in.-thick ablating carbon-phenolic over the capsule, it was shown that 0.20-in.-thick rubber was required to maintain the salts below 3,000°F. As previously stated, this is an upper limit.

These analyses showed that the capsule thickness would have to be greater than 0.050 in. and probably closer to 0.20 in. when accounting for the charred capsule condition. These thicknesses are too great to allow definition of the ablated surface depth to within ±10% at the time of salt vaporization and, hence, salt injection into the exhaust stream.

As discussed previously, Union Carbide Grafoil was selected as the most desirable material based on the thermal stability at elevated temperatures, the low permeability characteristics, and the reduced thermal conductivity normal to the Grafoil surface. Thermal analyses which were conducted with this material showed that a 0.010-in.-thick Grafoil layer insert would be sufficient to maintain the salts below 3,000°F up to time of exposure. This configuration provided the desired accuracy of releasing the salts within ±10% of the alloted surface depth for the area ratios considered.

4. LABORATORY TESTS

a. Specimen Design and Fabrication

Based upon the previously discussed selection of tracer and capsule materials and thermal analysis, laboratory specimens were designed and fabricated. The specimens were designed using MX4926 carbon-phenolic which represents the maximum thermal penetration and, hence, the most challenging for proper containment of the tracers up to time of injection.

The specimens were fabricated from flat laminate moldings of MX4926 carbon-phenolic which were machined to approximately 1.0-in. outside diameter (see figure 2). A 0.3-in.-diameter hole was bored into the specimen into which a 10-mil preformed Grafoil capsule was inserted. The tracer salts were installed in this capsule and a phenolic plug was bonded into the cavity backside.

The specimens were instrumented with three W5Re/W26Re thermocouples to define the thermal profile through the specimen and capsule during test. Two of the thermocouples were installed in the carbon-phenolic above the capsule and one was installed in the capsule in direct contact with the inner surface of Grafoil. This latter thermocouple defined the time when the salts were actually exposed to the exhaust flame. The thermocouple

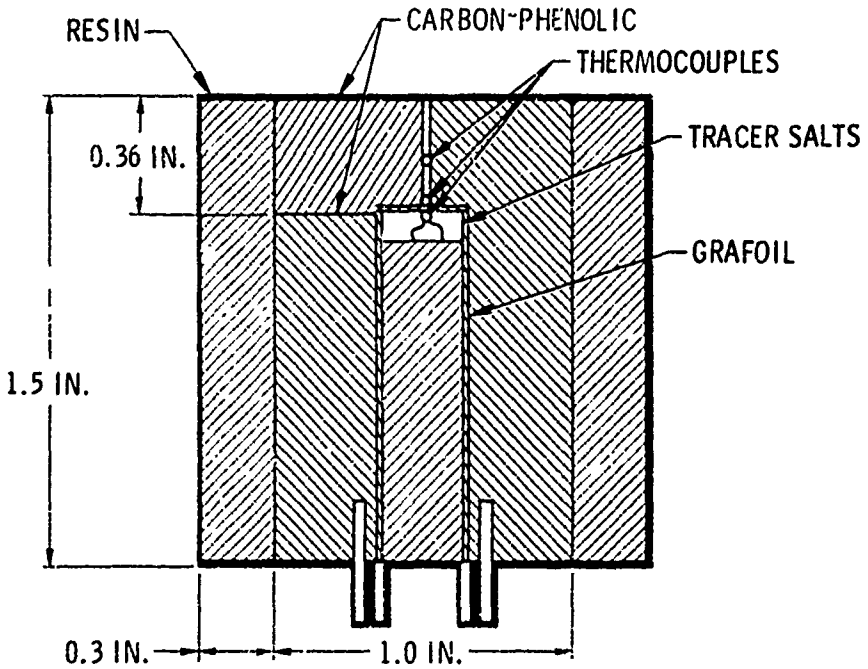

Figure 2. Tracer Salt Capsule
(Laboratory Specimen)

leads were routed around the capsule to instrumentation pins installed in the specimen. The entire capsule was encased with an epoxy resin to provide thermal protection for the leadwires and reduce the two-dimensional thermal transfer effects over the face of the specimen.

b. Test Setup

The specimens were subjected to a high heat flux, ablating environment generated with the plasma-arc torch in the UTC Engineering Laboratories, Sunnyvale, California. This torch uses a gaseous mixture of 95% argon and 5% hydrogen with a flow rate of 2 ft^3/min. A temperature of approximately 10,000°F can be generated in the torch; however, the actual temperature environment imposed on the specimen was reduced considerably, probably in the temperature range between 5,000° and 6,000°F. Several exploratory tests were made to define the angle of flame impingement to obtain a high rate of ablation. An orientation of approximately 45° to the specimen surface was chosen as being most representative of high ablation coupled with a high thermal input to the specimen. This provided an approximate simulation of the nozzle environment where the surface is experiencing ablation plus in depth heating rather than solely thermal penetration. No attempts were made to accurately simulate the magnitude of the total heat flux input or ablation as would be encountered in the actual nozzle system.

A preliminary test was conducted on an identical specimen without the salts or instrumentation to demonstrate the carbon-phenolic was uniformly ablated at a sufficiently high rate. This test demonstrated the surface was ablated at approximately 3 mils/sec.

A spectrograph camera was modified for detection of the salt release in the laboratory tests. The modifications consisted of adapting the lens system for a relatively short focal length (4 to 10 ft). This modification was necessary because the instrument had been used to view a rocket plume from distances up to 3,000 ft.

Attempts were made to use infrared-sensitive film to detect the tracer salt ejection. This technique proved unsuccessful since the plasma torch exhaust plume is detectable in the infrared spectrum and completely masks out the salt tracers.

The thermocouple output was recorded on oscillograph recorders.

c. Description and Result of Thermocouple Tests

Four specimens were tested with the plasma-arc torch. Three of the specimens contained lithium fluoride as the trace element, and the fourth contained cesium sulfate. The thermocouples were numbered consecutively 1 through 3 with No. 1 being nearest the surface.

Test No. 1 was terminated prematurely at 123 sec due to communication difficulties. The specimen was allowed to cool to ambient temperature and the test was rerun. Figure 3 shows the thermocouple data for this sequence. The test continued for another 95 sec at which time the bond failed on the removable portion of the top of the specimen, thereby exposing the capsule which ruptured immediately. Spectrographic measurements indicate that the salts were injected into the flame 30 msec before thermocouple No. 3 indicated the capsule had ruptured.

Thermocouples Nos. 1 and 2 were in the virgin carbon-phenolic which allowed the heat flux to be calculated provided the capsule failed prior to exposure to the flame. The signals became erratic prior to exposure since the resin around the outer periphery of the specimen ablated and exposed the leadwires. The leadwires for thermocouple No. 3 were routed through the capsule which protected them until after the capsule ruptured.

The erratic nature of thermocouple No. 3 toward the end of the test (dotted line in figure 3) is believed to be caused by the loss of intimate contact with the Grafoil. This thermocouple was bonded to the Grafoil with a graphitic adhesive which has a maximum temperature capability of 1,400^{o}F. Once this contact is lost, the thermocouple measures the thermal response of the tracer salts. The temperature inside the capsule was low until sufficient heat was transferred to melt the salts, which may explain the apparent anomaly in the last 26 sec of the test.

For subsequent tests, the specimen was reorientated in the test apparatus to prevent early ejection of the upper portion of the specimen. Test No. 2 was terminated erroneously just before the capsule was exposed; however, the spectrograph film indicated that the salt had not been injected into the flame during the test. This test provided further justification for the belief that the capsule was retaining the salts up to time of exposure.

Test Nos. 3 and 4 were conducted without the termination problems encountered previously, and again demonstrated the capsule design. Figure 4 shows the thermocouple data for test No. 3.

Thermocouple Nos. 1 and 2 again became erratic prior to their exposure. Thermocouple No. 3 maintained continuity until approximately 68 msec after the spectrograph indicated that the salts had been injected.

The thermocouple tests were recorded with an oscillograph, a spectrograph, and high-speed motion picture photography. Timing marks were placed on each record with a signal generator at 1-sec intervals. In addition, correlation marks also were placed on each recorder with a circuit that was activated at 30-sec intervals. Due to the intensity of the flame, motion pictures were not able to detect the injection sequence of the salts.

These laboratory tests demonstrated that the capsule design retains the salts until the surface recedes exposing the capsule. The thermocouple data indicated the salts were ejected within +30 to -68 msec from the time of capsule exposure, which is well within instrumentation accuracy. Based upon these results, the in-situ ablation detection concept utilizing metallic salts was considered acceptable for full-scale demonstration test firings.

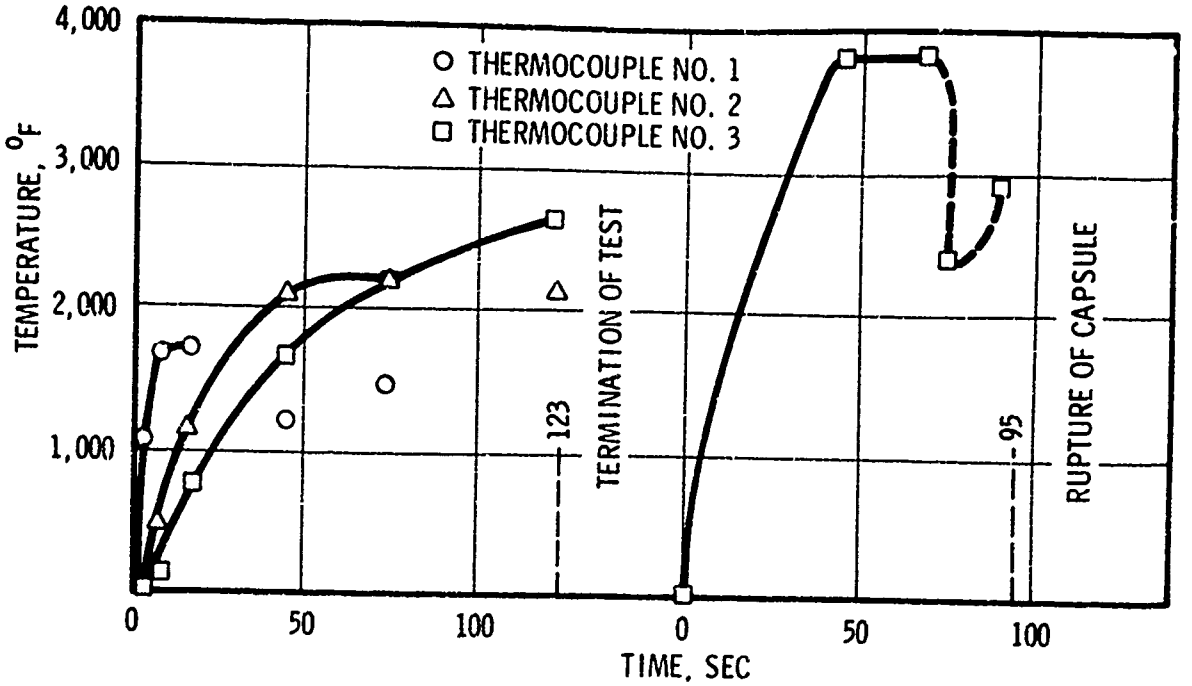

Figure 3. Thermocouple Data Laboratory Tests 1 and 1A (Lithium Fluoride)

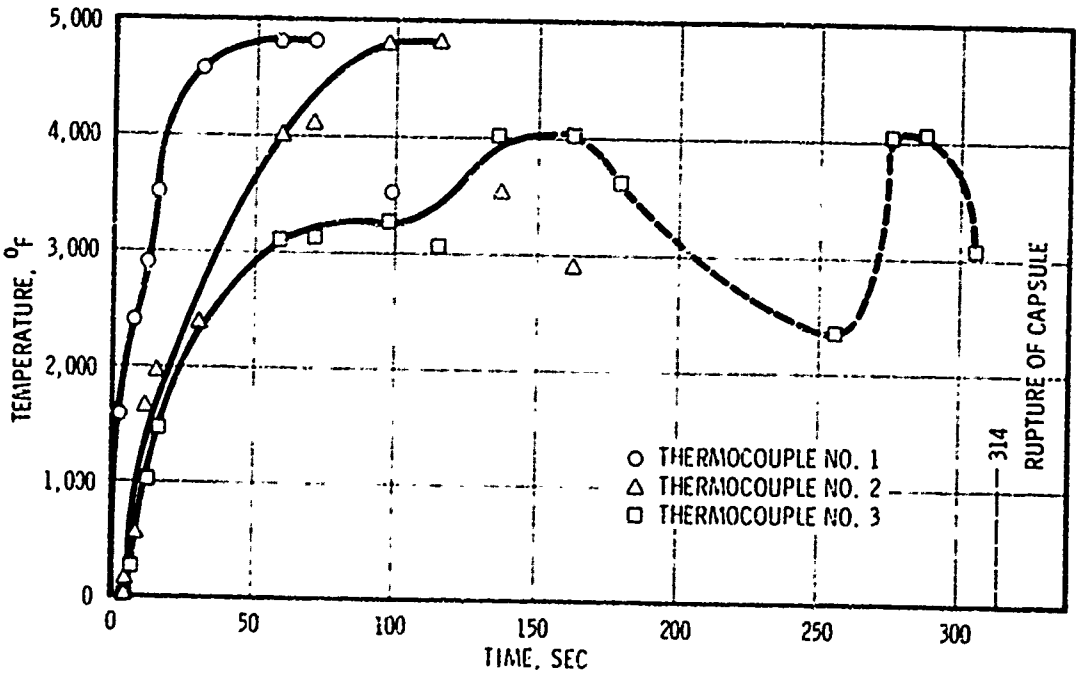

Figure 4. Thermocouple Data Laboratory Test 3 (Lithium Fluoride)

SECTION VI

PHASE II - NOZZLE DESIGN AND EVALUATION

1. NOZZLE DESIGN

One basic nozzle design using two different hotside materials was made. The configurations were designed to meet the requirements presented in table III. One design (S/N 01) used a monolithic insert fabricated from a carbon cloth phenolic flat laminate, Fiberite Corp. MX4926 (figure 5). The other design (S/N 02) used a three-piece flat laminate silica-phenolic (Fiberite MX2600) part with a codeposited silicon carbide/pyrolytic graphite throat insert package (figure 6). The coating thickness was a nominal 0.06 in. An ATJ substrate was used. The insert was fabricated by Atlantic Research Corp. The codeposited silicon carbide/pyrolytic graphite throat insert was backed with an ATJ graphite heat sink. A 10-mil-thick piece of Union Carbide 6TB Grafoil (70 lb/ft^3 density) was installed between the throat insert and backup ATJ to minimize the coating compressive stresses by allowing the throat insert to grow radially during insert heating. A Graph-i-tite G-90 washer was used forward of the throat insert to prevent undercutting of the pyrolytic-graphite coating.

The entrance cap was fabricated by troweling in V-61 insulation. The nozzle was designed this way so the entrance could be blended smoothly into the aft closure insulation without fabricating close tolerance components. The entrance cap was troweled into the nozzle at AFRPL after the nozzle was assembled into the aft closure. A GFE mild steel shell supported the phenolic components and attached to the 36-in. CHAR motor. A steel retention plate was used to restrain the throat ejection load and hold the ablative liner in the steel shell.

TABLE III

NOZZLE DESIGN REQUIREMENTS

Throat diameter, in.	2.3
Expansion ratio	7
Maximum chamber pressure, psia	800
Maximum burn time, sec	30
Theoretical flame temperature, ^{o}F	5,700
Propellant	UTP-3001 (16% aluminized, 84% solids-loaded PBAN composite)

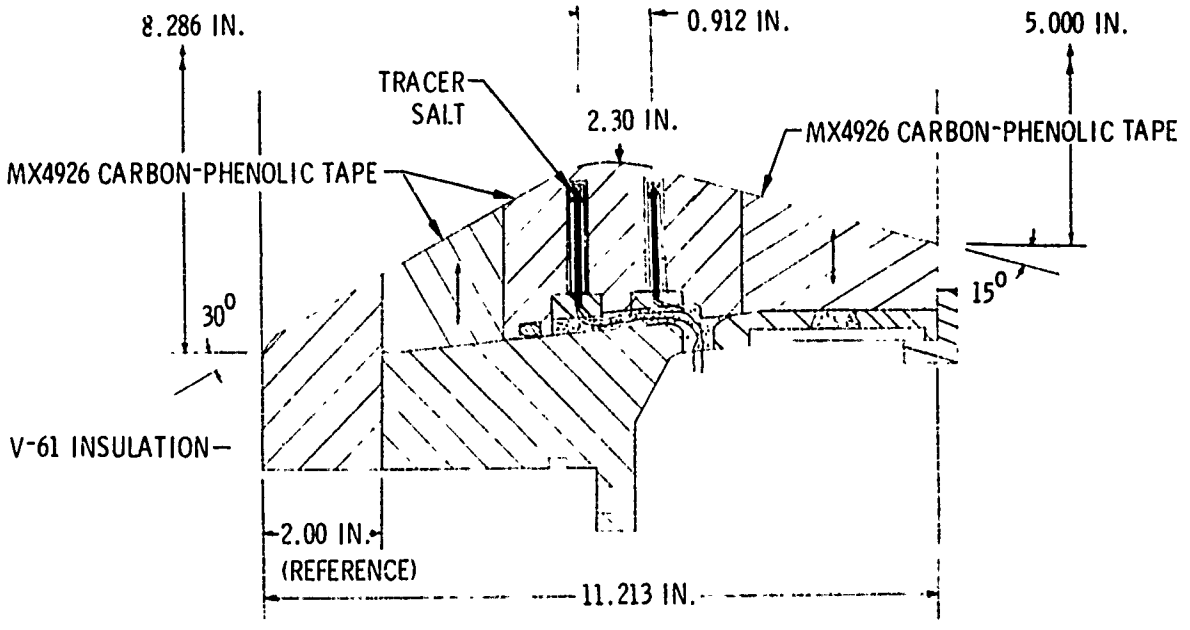

Figure 5. Carbon-Phenolic Nozzle Assembly S/N 01

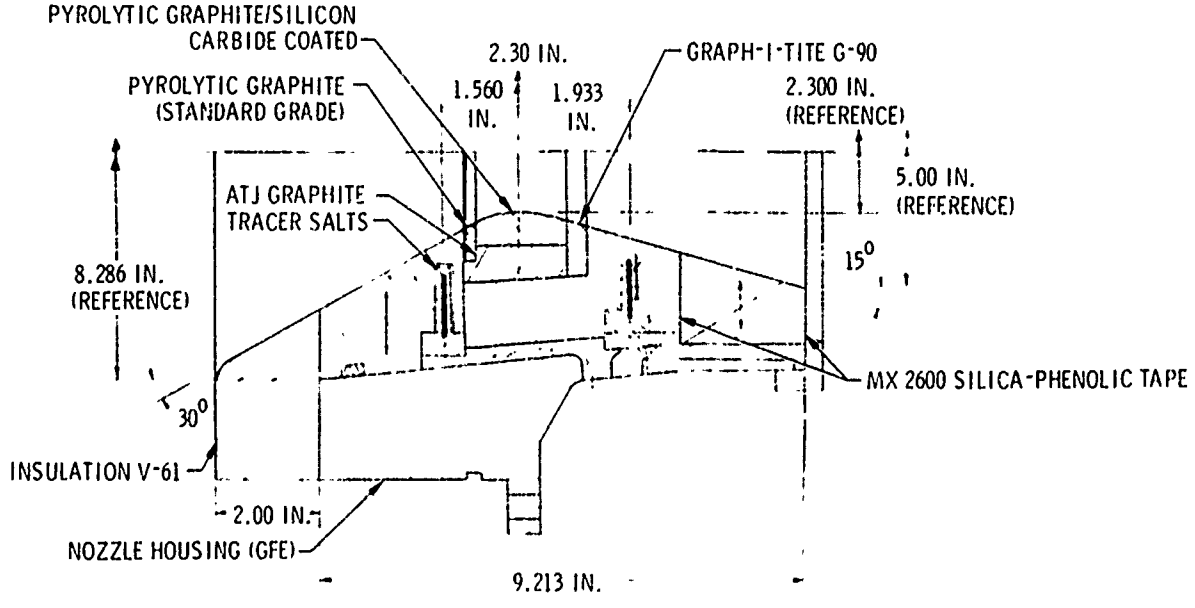

Figure 6. Silica-Phenolic Nozzle Assembly S/N 02
with Pyrolytic-Graphite-Coated Throat

2. NOZZLE ABLATION RATE PREDICTION

The predicted ablation rates for the carbon- and silica-phenolic nozzle materials were made using an empirical correlation based on Titan III data. It was originally planned to perform a surface regression prediction analysis using the equilibrium surface thermochemistry and charring material ablating programs since the propellant to be used was an uncured PBAN formulation. The propellant was changed to a cured grain using UTP-3001b formulation. This propellant is the same formulation from which the empirical correlation data were derived. Since the anticipated chamber pressure (800 psia) was very close to that of the Titan III (668 psia average) from which the data were obtained, the empirical correlation was deemed most accurate and usable for this program.

The predicted ablation data using the empirical correlation are as follows:

Nozzle Material	Area Ratio	Mach No.	Ablation Depth, in.	Average Ablation Rate, mils/sec
Carbon-phenolic	-2.08	0.3	0.171	5.3
	+1.98	2.0	0.096	3.0
Silica-phenolic	-2.08	0.3	0.183	5.7
	+1.98	2.0	0.162	5.1

Posttest analysis of nozzle S/N 01 revealed that the nozzle materials eroded at approximately 30% to 40% of the rate that had been predicted. Therefore, the capsules located in the subsonic and supersonic locations at depths of 0.150 and 0.195 in., respectively, were not exposed. The reasons for this reduced ablation is not clearly understood; however, the following factors are considered prime contributors. The most probable reason for this ablation decrease is due to an expanding and cooling of the boundary layer by the introduction of the ablated V-61 insulation upstream from the nozzle. Such a phenomenon was observed in a NASA program for studying the effects of liquid injection thrust vector control on low-cost ablatives (Contract No. NAS3-13304) which was conducted recently at UTC. In that program, the ablation rate of silica-phenolic was decreased by as much as 50% of that predicted by the presence of rubber upstream from the nozzle. For this particular test, it is difficult to estimate the amount of rubber ablation with any degree of accuracy since the insulation was trowelled into the aft closure after the nozzle was installed and a prefire profile was not obtained.

A secondary effect may be that the empirical correlation is based on test data of sufficient duration (120 sec) so that the ablative surface temperature has reached a more nearly equilibrium condition for a major portion of the firing. The temperature keeps increasing throughout the firing; however the major transients are encountered prior to 20 to 25 sec. For the shorter duration firing (30 sec) the average surface temperature throughout the firing is considerably lower; therefore, a reduced average ablation rate is encountered.

The depths of the tracer capsules for nozzle S/N 02 were modified by correcting the original predictions by the ratio of the actual ablation on nozzle S/N 01 to that which was predicted. These depths of the capsules below the surface

were arbitrarily decreased by an additional 5%, which was considered to ensure ejection during the firing. However, only two of the tracers were exposed during the firing even with the additional conservatism. A summary of the salt locations below the surface for both nozzles is presented in table V.

3. INSTRUMENTATION DESIGN

The test nozzles were instrumented to define the accuracy of surface recession measurement as detected by the passive tracers. Thermocouple plugs were installed at the same area ratio as the passive tracers to determine the chronological in-depth temperature history of the ablative part. Two thermocouple plugs were used, one in the subsonic region and one in the supersonic region. These thermocouple plugs were proven to be quite reliable on Contract No. F04611-69-C-0065; therefore, the same type of thermocouples (W5Re/W26Re) were used. Each thermocouple plug contained five individual thermocouples at various depths. Table IV shows the depths of thermocouples for the subsonic and supersonic regions for both nozzles. Two different salt tracers were used in the same axial location as the thermocouple plugs. Figure 7 shows the relative location of the two tracer capsules and the thermocouple plug. The salt capsule design is detailed in figure 8 which is the same basic design tested and proven during phase I laboratory tests. The quantity of salts, location, and orientation of each capsule for both nozzles is summarized in table V.

4. NOZZLE FABRICATION

The ablative components for both nozzle designs were fabricated by molding flat laminates of the phenolic cloth at approximately 2,000 psia and 320° for 2 hr.

For ease of fabrication, the ablative components were made in three parts with bonded joints forward and aft of the throat. The carbon-phenolic bonded assembly was then machined as one piece. The silica-phenolic was partially machined before bonding so the throat insert could be installed. Ten mils of Grafoil were bonded to the backside of the codeposited silicon carbide/pyrolytic graphite before installation in the ATJ insulator.

TABLE IV

SUMMARY OF THERMOCOUPLE DEPTH

Nozzle S/N	Initial Area Ratio	Thermocouple No.	Prefire Depth Below Surface, in. Subsonic	Supersonic
01	1.1	1	0.031	0.031
01	1.1	2	0.109	0.107
01	1.1	3	0.175	0.185
01	1.1	4	0.247	0.263
01	1.1	5	0.324	0.326
02	2.0	1	0.087	0.065
02	2.0	2	0.151	0.115
02	2.0	3	0.190	0.171
02	2.0	4	0.299	0.241
02	2.0	5	0.399	0.396

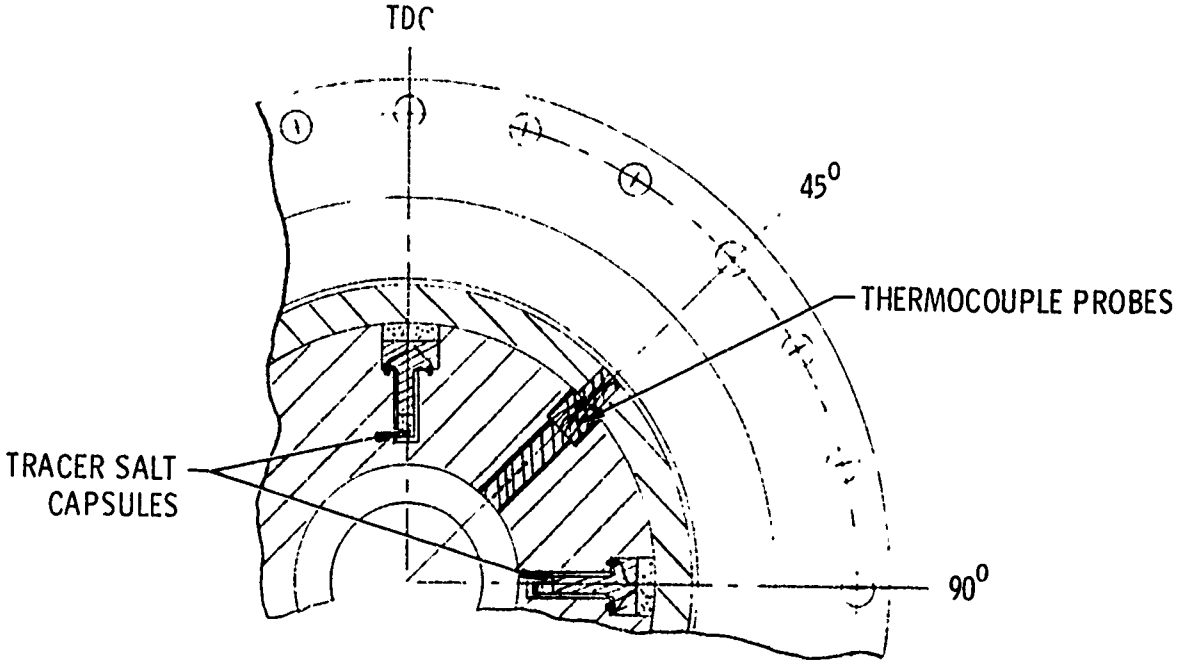

Figure 7. Tracer Salts and Thermocouple Probe Locations

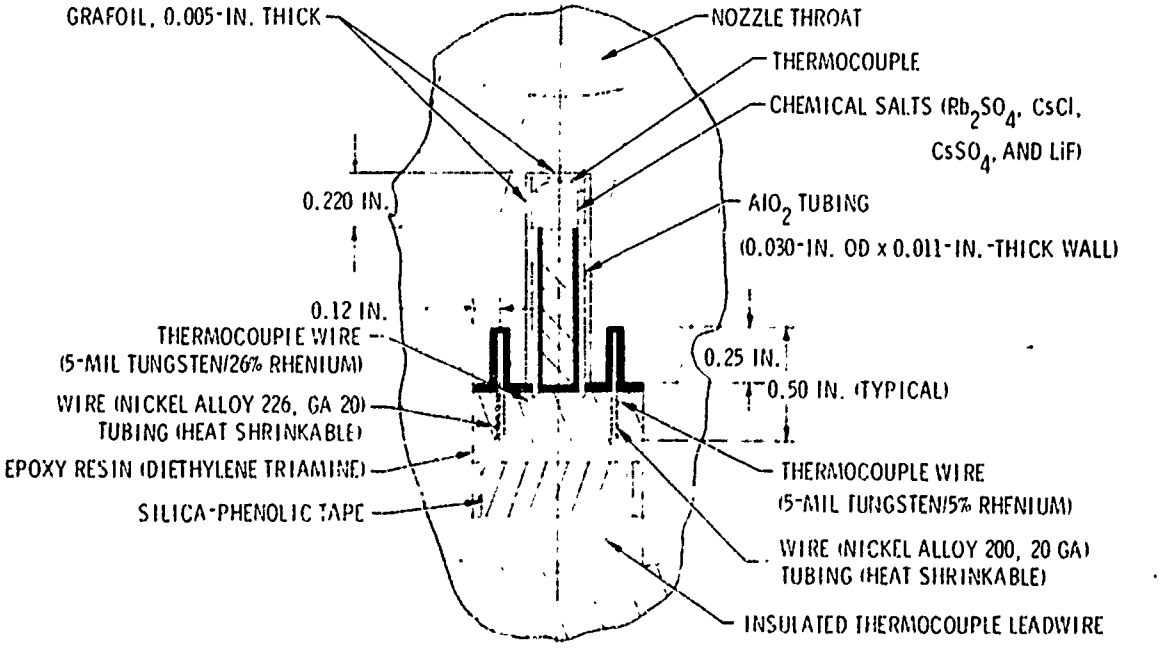

Figure 8. Tracer Salt Capsule with Thermocouple

TABLE V

SUMMARY OF TRACER SALT CAPSULE DATA

Nozzle S/N	Capsule Location	Orientation*	Tracer Salt	Quantity of Salt, g	Depth Below Surface, in.
01	Subsonic	90°	Rubidium sulfate	1.01	0.060
01	Subsonic	180°	Cesium sulfate	1.32	0.150
01	Supersonic	TDC	Rubidium sulfate	1.139	0.195
01	Supersonic	90°	Lithium fluoride	0.54	0.086
02	Subsonic	180°	Rubidium sulfate	1.384	0.225
02	Subsonic	90°	Cesium sulfate	1.041	0.165
02	Supersonic	90°	Rubidium sulfate	1.345	0.110
02	Supersonic	TDC	Lithium fluoride	0.310	0.160

*Angular location (clockwise), aft looking forward.

The holes for the encapsulated salts and thermocouple plugs were machined from the outside surfaces. The Grafoil, thermocouple wires, and salts were installed in these predrilled cavities. The remaining backside hole was plugged with a rod molded from the parent material. The phenolic plug provided ablation resistance once the capsule cavity is exposed. The thermocouple plugs were bonded in the holes between the two salt capsules at 45°. The thermocouple plugs were purchased from Aerotherm Division of Accurex Corp.

The assembly was then bonded in the steel shell. The thermocouple leads were fed through holes in the steel shell via milled slots in the phenolic components. The slots were filled and sealed with epoxy.

The complete record of each nozzle assembly was documented in the Quality Control log book.

5. TEST DESCRIPTION

The nozzles were tested on the 36-in.-diameter CHAR motor at AFRPL. UTC furnished the nozzle assembly, a streak spectrograph, modified Jarrell Ash laboratory spectrograph, and test liaison personnel. AFRPL furnished all the propellant grains, associated motor hardware test tooling and stands, basic recording instrumentation, test personnel, photographic coverage, and data acquisition and reduction. The test motor was fired in a vertical position (nozzle up) on pad No. 2 of the solid rocket test area 1-32 at AFRPL.

The test motors were instrumented with 14 thermocouples (W5Re/W26Re) and two 1,500-psi Taber pressure transducers. Axial thrust measurements were obtained using the AFRPL six-component stand.

The thermocouples were recorded on the standard digital instrumentation.

The propellant used was a PBAN formulation using a 16% aluminized, 84% solids load (UTP-3001). The burning rate at 1,000 psia was 0.385 in./sec at 80°F with a pressure exponent of 0.25.

Two instrumentation methods of detecting the tracer characteristics in exhaust plumes were used: (1) a UTC-owned streak spectrograph which records the data photographically, and (2) a modified Jarrell Ash laboratory spectrograph, which is an Air Force owned spectrographic measurement system under Contract No. F33615-69-C-1269. The streak spectrograph operates as a transmission spectrograph and displays the 0.4 and 0.9 wavelength region of the spectrum on a continuously moving 5-in.-wide film.

The streak spectrograph, shown schematically in figure 9, consists of a 508 mm f/5.6 objective lens, a focusing system composed of a flip-up mirror and ground glass screen, an adjustable slit assembly, a 178 mm f/2.5 collimating lens, and a surplus K-46 Navy aerial camera. In some cases an optical image rotator is placed in front of the objective lens to orient the plume axis with the slit. The apparatus is mounted on a base so that the camera and the front optical

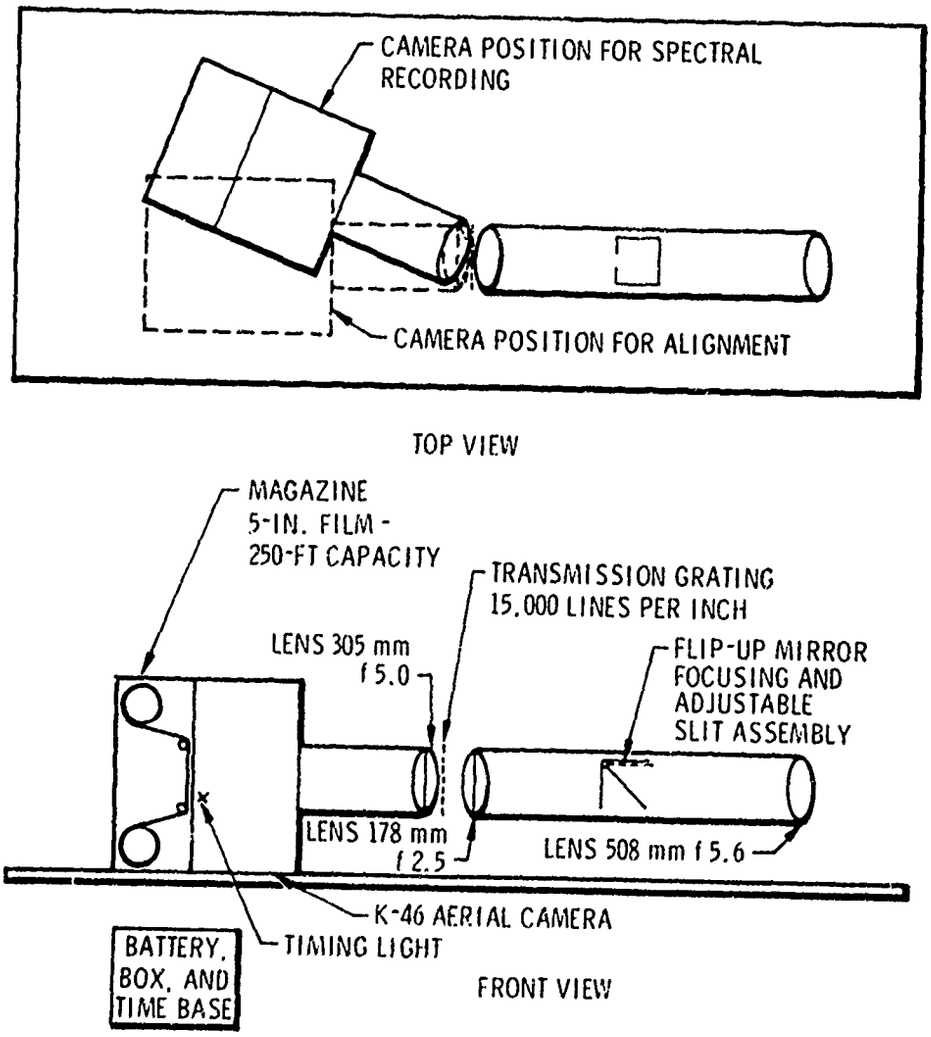

Figure 9. Schematic of Low-Resolution Streak Spectrograph

assembly can be initially aligned and focused on the target. The camera is then placed at the appropriate angle to display the spectral region of interest at the film plane.

The combination of the 15,000 lines/in. transmission grating and a 305-mm lens creates a dispersion of 0.1345 micron/in. in the first order spectrum and, as normally used, displays the 0.4 to 0.9 micron wavelength region on the film. The K-46 aerial camera utilizes 250-ft spools of 5-in. Kodak 2424 (Estar Base) aerographic film and is capable of streak rates from 0 to 7 in./sec. A timing light slaved to an external timer applies a time base to the film. The slit, adjustable in width and height, is located at the focal plane of the objective lens. The light from the slit, rendered parallel by the collimating lens, passes through the grating and is focused on the film plane by the imaging lens. A set of batteries or power supply provides 30 v to operate the film transport motor and the time base system.

The time resolution of the streak spectrograph is a function of the slit height and the film lineal speed. The latter must be chosen in accordance with the slit width and the photographic sensitivity of the film. Present experience indicates that for films with ASA ratings greater than 100 and with a slit 200 microns wide and 0.2 in. long, time resolution is less than 0.1 sec.

The modified Jarrel Ash spectrograph consists of a trailer-mounted 1.5-m Wadsworth grating spectrograph equipped with a set of photo tubes and slit assemblies positioned at the characteristics spectral lines of the tracers used and a device to sweep a narrow band of the spectrum past the slits. The time of arrival of the tracers in the plume is determined by recording the output of the photo multiplier tubes. With a sweep rate of 4/sec, the time of arrival of a tracer can be resolved to within 0.25 sec.

a. Test No. 1 (S/N 01)

The test was conducted at a maximum chamber pressure of 750 psi with a web time of 30.8 sec as shown in figure 10. Visual observations indicated the motor fired properly but the cesium salt capsules in the subsonic region and both capsules in the supersonic region were not exposed. Results from the streak spectrographic camera confirmed that only the rubidium sulfate at the subsonic location had been injected into the exhaust plume.

The Jarrell Ash spectrograph did not give any signal for the rubidium which was ejected. The remainder of the nozzle was in good condition.

b. Test No. 2 (S/N 02)

The test was conducted at a maximum chamber pressure of 765 psi with a web time of 30.0 as shown in figure 11. Visual observation indicated the motor fired properly but the rubidium sulfate capsule in the

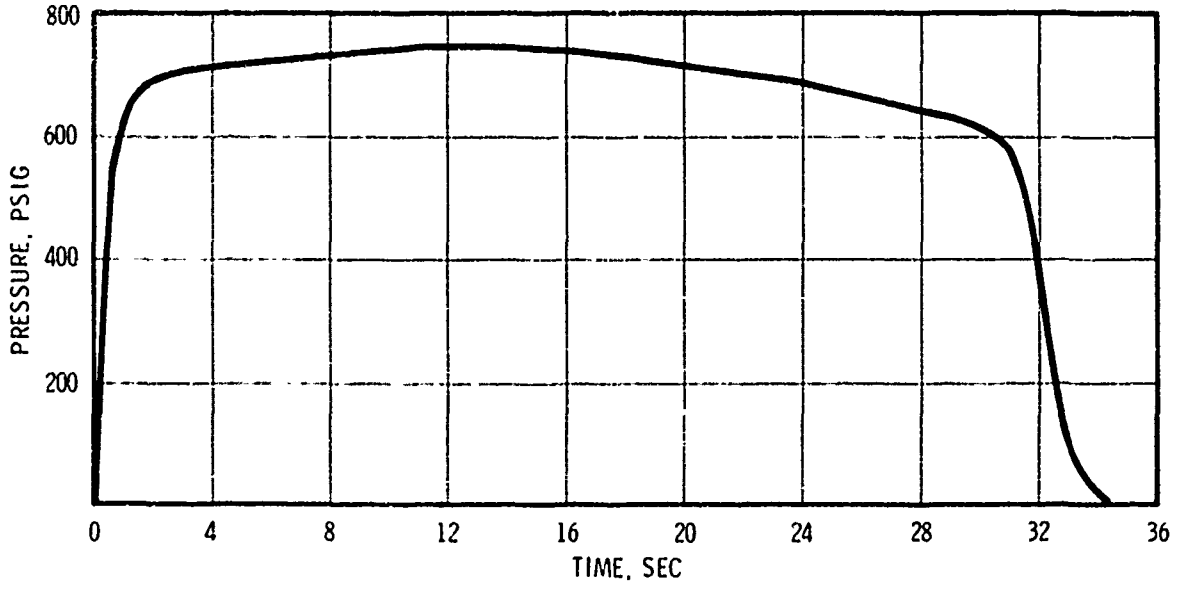

Figure 10. Carbon-Phenolic Nozzle S/N 01 Duty Cycle

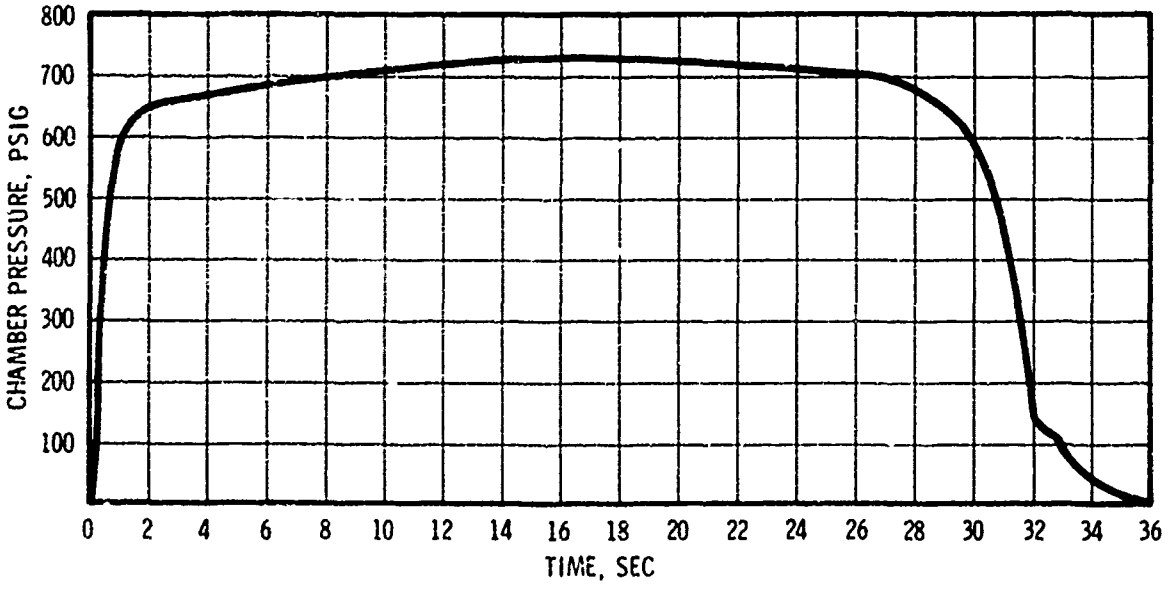

Figure 11. Silica-Phenolic Nozzle S/N 02 Duty Cycle

subsonic region and the lithium capsule in the supersonic region were not uncovered. Results from the streak spectrographic camera confirmed that cesium from the subsonic region and rubidium sulfate from supersonic region were injected into the exhaust plume. The Jarrell Ash spectrograph was not used on the second firing since it failed to provide any signal on test No. 1. Visual inspection revealed the nozzle was in good condition. The codeposited silicon carbide/pyrolytic-graphite coating appeared to be in excellent condition.

SECTION VII

PHASE II - POSTTEST ANALYSIS

Posttest analyses were conducted on both test nozzle assemblies. The throat materials were carbon-phenolic and codeposited silicon carbide/pyrolytic graphite. A summary of the pretest and posttest throat measurements are shown in table VI. The carbon-phenolic throat erosion was not uniform, which was anticipated with an ablative configuration. The codeposited throat eroded evenly with an average erosion rate of 0.8 mil/sec.

The nozzle assemblies were disassembled, the ablative components were sectioned, and measurements were made for surface ablation and char depth. The data are presented in table VII. No corrections were made due to char swell or the inherent error due to allowable design tolerances.

A summary of the thermal penetration data in the nozzle materials for both nozzles as recorded by the thermocouple plugs is presented in tables VIII and IX.

1. CORRELATION OF SALT DETECTION IN EXHAUST PLUME WITH CAPSULE THERMOCOUPLE

The temperature history recorded from the thermocouples embedded in the tracer salts and the chamber pressure-time traces for test S/N 01 and S/N 02 are shown in figure 12. The temperature indicated by each thermocouple started increasing shortly after ignition,* with the rate depending on the depth of the tracer, and continued to rise until either a transition or melting point of the tracer salts was reached or the thermocouple was exposed to the combustion gases. The temperature decrease upon melting of the cesium and rubidium salts is not understood; however, contamination of the melt with decomposition products from the salt or evaporative cooling from the cavity could cause the decrease in temperature. For purposes of this program the important function of the thermocouple was to indicate the time at which the tracer from the cavity was expelled into the gas stream. This was taken to be the time when the thermocouple indicated a very sharp change in temperature or became extremely erratic indicating wire burnthrough. Figure 12 shows that three of the eight tracers in the two nozzles were released into the combustion gases.

The data show that whenever the thermocouple data indicated that a tracer was released into the exhaust gases, it was detected by the spectrograph in the plume. In all cases the postfire observation of the nozzle supported the data. In test S/N 01 the time the tracer appeared in the plume agreed very favorably with the indicated time of release (3.99 versus 4.00 sec). For test S/N 02 the indicated time of arrival in the plume is approximate because of a failure of the timing light in the streak spectrograph. The estimated times presented in table X were determined by dividing the streak spectrograph record into equal time intervals such that the total time agreed with the pressure-time trace. These time estimates are not exact and the correlation between the thermocouple and streak spectrograph records which are indicated by these data are not as accurate as desired.

*In test S/N 02 the thermocouple in the lithium fluoride located in the supersonic section of the nozzle malfunctioned.

TABLE VI

PRETEST AND POSTTEST THROAT DIAMETERS

	Nozzle S/N	
	01	02
Pretest throat diameter, in.		
Minimum	2.297	2.299
Maximum	2.297	2.299
Posttest throat diameter, in.		
Minimum	2.435	2.336
Maximum	2.485	2.359
Average diameter erosion, in.	0.163	0.049
Erosion rate, mils/sec	2.7±0.3	0.8±0.2

TABLE VII

SUMMARY OF EROSION DATA AT TRACER SALT LOCATIONS

Nozzle S/N	Material	Area Ratio	Average Erosion Depth, in.	Erosion Rate mils/sec	Char Depth in.
01	MX4926	-1.1	0.106	3.4	0.415
02	MX2600	-2.0	0.210	7.0	0.143
01	MX4626	+1.1	0.078	2.5	0.430
02	MX2600	+2.0	0.090	3.0	0.245

TABLE VIII

THERMAL PENETRATION OF CARBON-PHENOLIC NOZZLE S/N 01
BASED ON THERMOCOUPLE PLUG READINGS

Thermocouple No.	Thermocouple Plug Location	Depth Below Surface (Prefire), in.	Pasttest Condition
1	Subsonic	0.031	Exposed 19.8 sec
2	Subsonic	0.109	Exposed 26.4 sec
3	Subsonic	0.175	Not exposed (33.0 sec at 3,275°F)
4	Subsonic	0.247	Not exposed (32.3 sec at 2,850°F)
5	Subsonic	0.324	Not exposed (34.3 sec at 2,100°F)
1	Supersonic	0.032	Exposed 17.9 sec
2	Supersonic	0.107	Not exposed (32.6 sec at 3,650°F)
3	Supersonic	0.185	Not exposed (33.0 sec at 2,875°F)
4	Supersonic	0.263	Not exposed (34.0 sec at 2,525°F)
5	Supersonic	0.326	Not exposed (36.0 sec at 2,000°F)

TABLE IX

THERMAL PENETRATION OF SILICA-PHENOLIC NOZZLE S/N 02
BASED ON THERMOCOUPLE PLUG READINGS

Thermocouple No.	Thermocouple Plug Location	Depth Below Surface (Prefire), in.	Pasttest Condition
1	Subsonic	0.087	Data invalid
2	Subsonic	0.151	Data invalid
3	Subsonic	0.190	Exposed 27.7 sec
4	Subsonic	0.299	Not exposed
5	Subsonic	0.399	Data invalid
1	Supersonic	0.079	Peaked after 31.1 sec at ≈4,050°F
2	Supersonic	0.115	Not exposed (2,725°F)
3	Supersonic	0.171	Data invalid
4	Supersonic	0.241	Data invalid
5	Supersonic	0.396	Data Invalid

TEST S/N 01

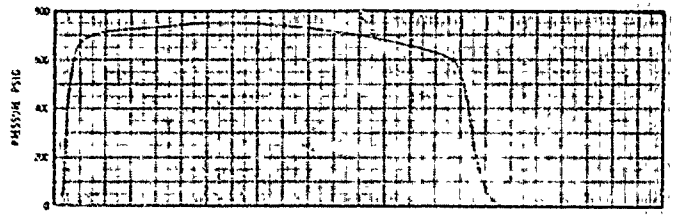

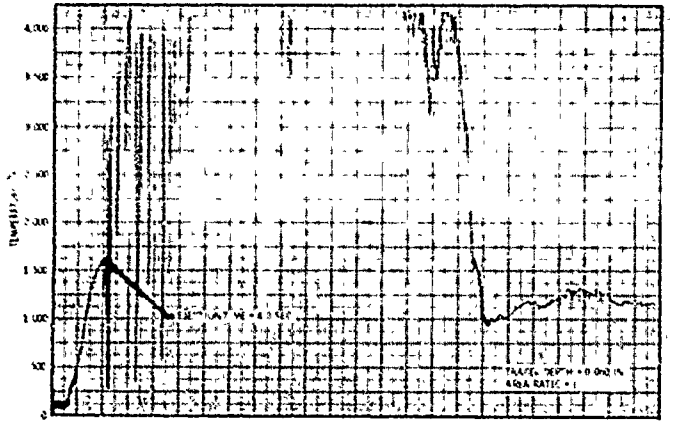

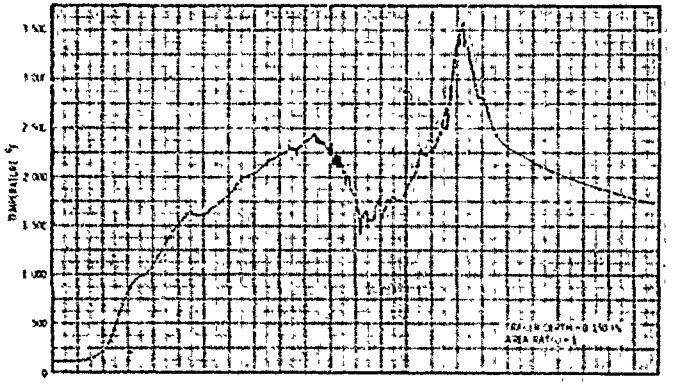

TEST S/N 02

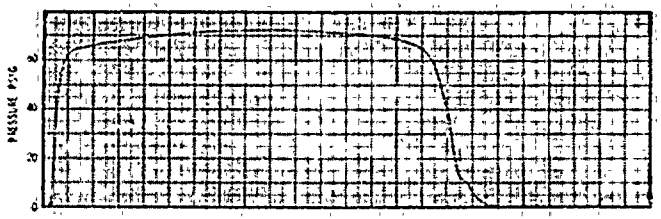

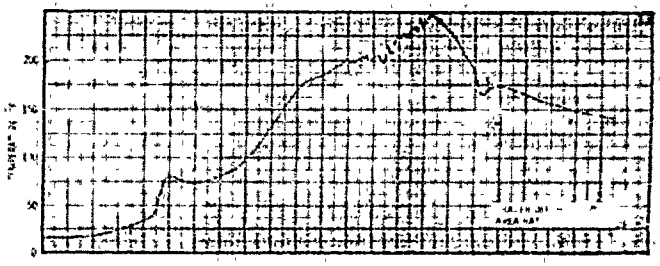

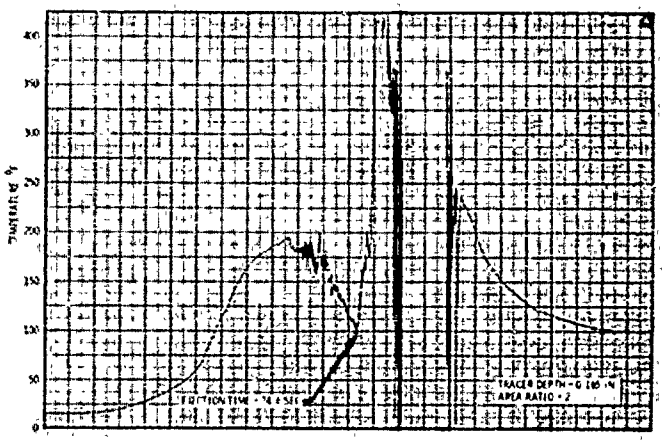

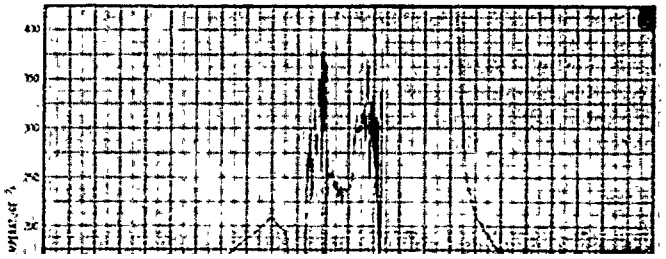

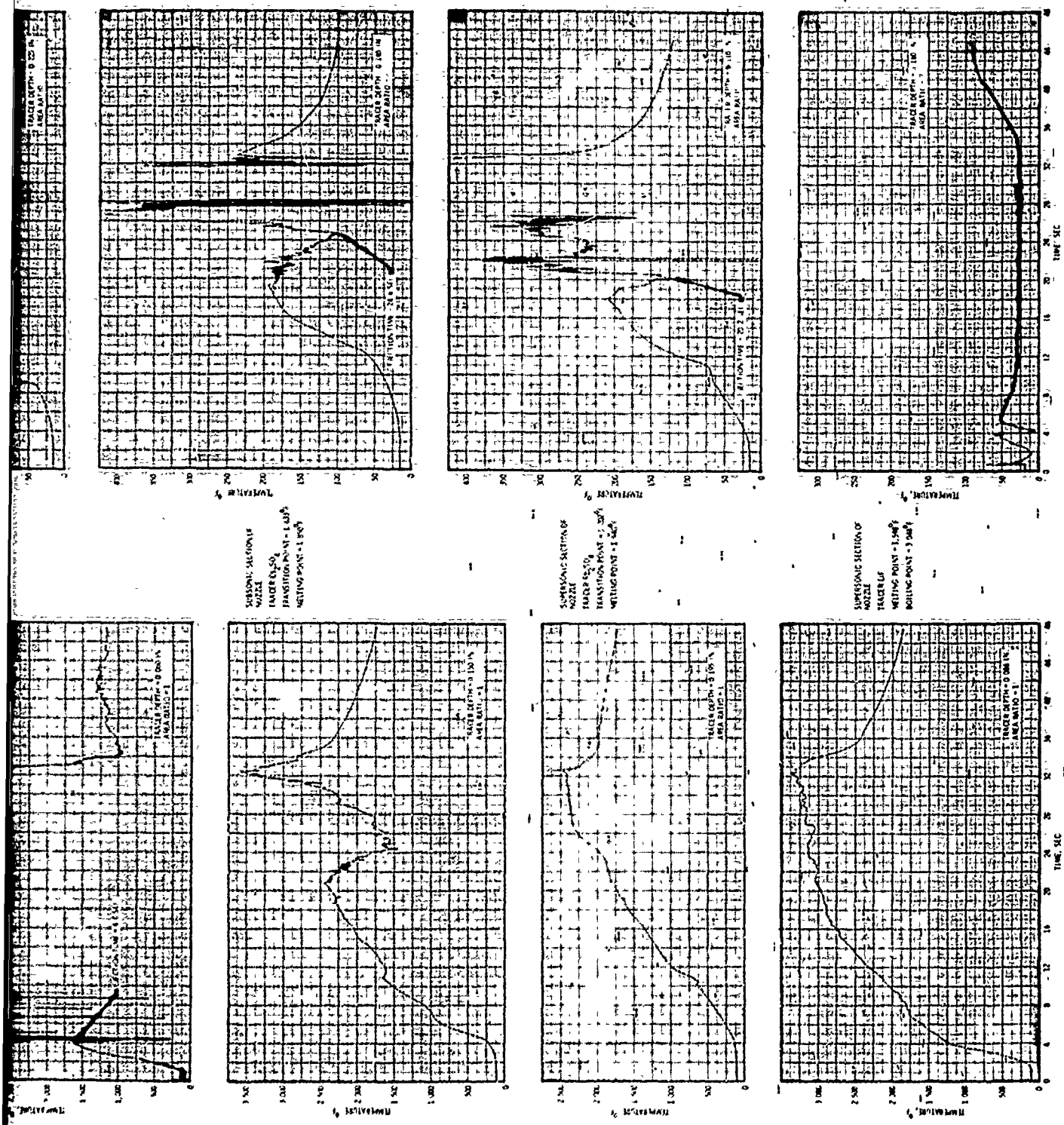

Figure 12. Temperature History of Spectroscopic Tracers and Chamber Pressure Time Trace

TABLE X

COMPARISON OF SPECTROGRAPH AND THERMOCOUPLE DATA WITH POSTFIRE OBSERVATION OF THE NOZZLE

Tracer	Spectrograph Time of Appearance		Tracer Thermocouple Time of Release		Postfire Observation: Did tracer Appear to Have Been Released?	
	S/N 01	S/N 02	S/N 01	S/N 02	S/N 01	S/N 02
Subsonic Rb_2SO_4	3.99	---	4.0	---	Yes	No
Subsonic Cs_2SO_4	---	25.4*	---	24.6	No	Yes
Supersonic Rb_2SO_4	---	19.5*	---	20.2	No	Yes
Supersonic Lif	---	---	---	---	No	Yes

*Estimate time based on run time from chamber pressure trace.

In addition to the spectrograph data presented in table X, the rubidium lines appeared at 28.75 sec in test S/N 01. Even though this appearance does not correlate with an indication of tracer release from the thermocouples, the temperature record for the subsonic rubidium sulfate tracer suggests a changing condition at that time. Postfire observation of nozzle S/N 01 indicated further that the rubidium sulfate tracer in the supersonic portion of the nozzle was nearly burned through and could also have been subliming, thereby introducing a small quantity of tracer element into the main flow.

2. CORRELATION OF CAPSULE AND PLUG THERMAL RESPONSE

The temperature history results recorded from the five thermocouples in the subsonic and supersonic areas of the phenolic nozzles and the prefired thermocouple depths are shown in tables VIII and IX. The surface history is obtained from the data when the thermocouple response becomes erratic, indicating that the thermocouple wire has been broken. The surface recession history for the carbon-phenolic nozzle S/N 01 in the subsonic and supersonic areas based on thermocouple readings are shown in figures 13 and 14, respectively. In figure 13, the capsule thermocouple was exposed at 4 sec and thermocouple Nos. 1 and 2 of the plug were exposed at 19.8 and 26.4 sec, respectively.

Since the capsule thermocouple and plug thermocouple No. 1 were at the same depth, the indication is that the salt was injected into the plume considerably earlier than desired. In figure 14, thermocouple No. 1, which was at a prefire depth of 0.032 in. was exposed at 17.8 sec, and a total erosion of 0.100 in. occurred at the thermocouple plug. However, the total ablation was only 0.079 in. at the capsule location and the capsule was not exposed.

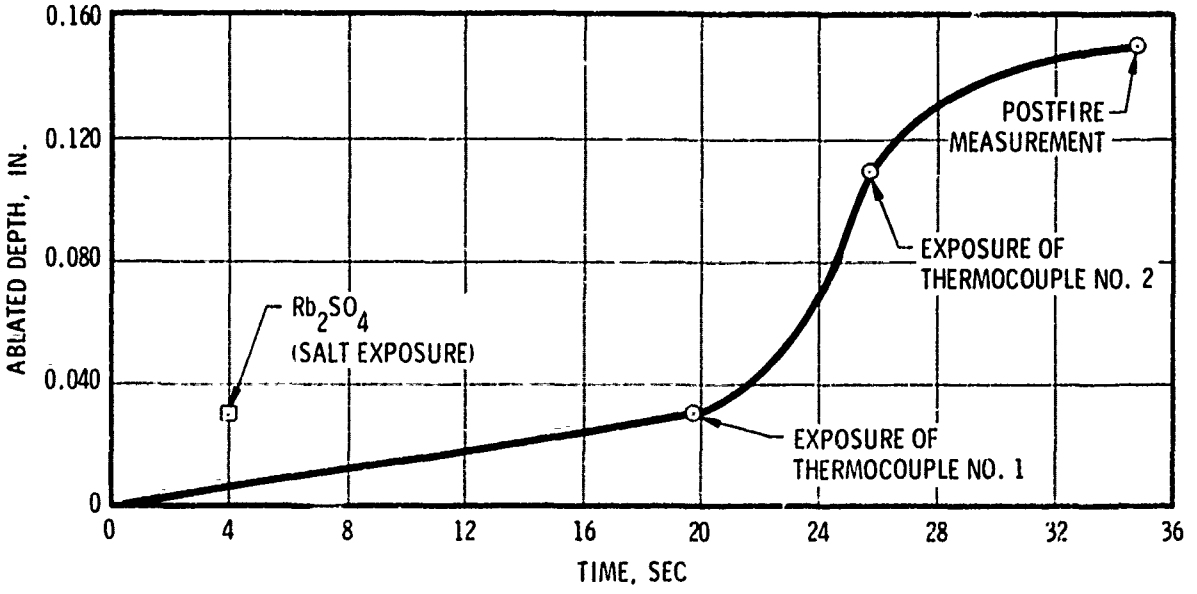

Figure 13. Surface Recession at Subsonic Thermocouple Plug Location, Carbon-Phenolic Nozzle S/N 01

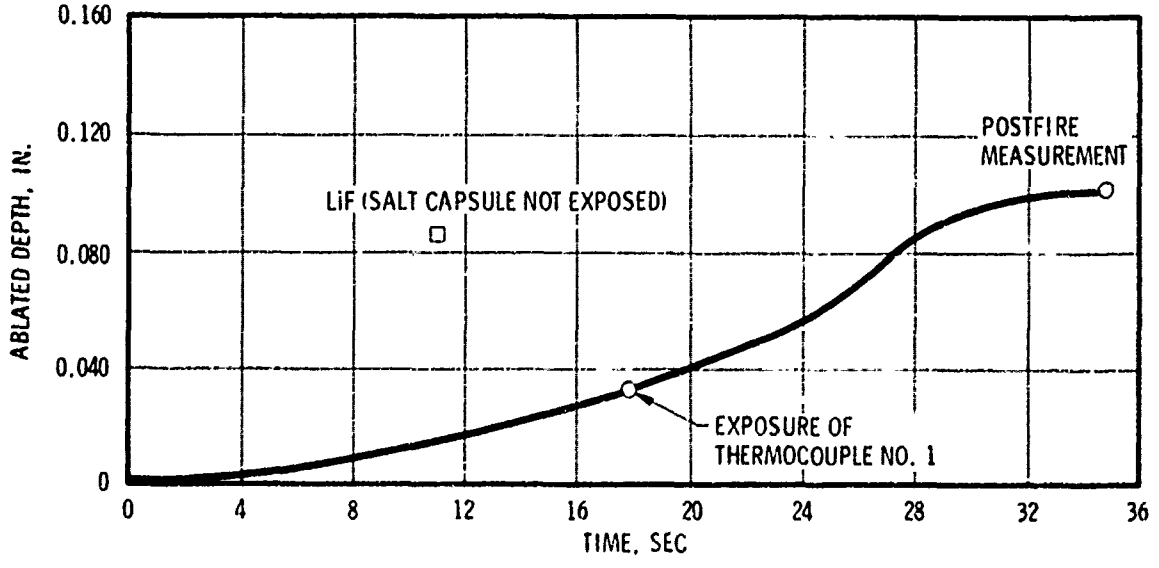

Figure 14. Surface Recession at Supersonic Thermocouple Plug Location, Carbon-Phenolic Nozzle S/N 01

The surface recession history for silica-phenolic nozzle S/N 02 in the subsonic and supersonic areas based on thermocouple readings are shown in figures 15 and 16, respectively. In figure 15, results for thermocouple Nos. 1 and 2 are not shown since no readings were obtained from the data. Based on the detection of the tracer salt in the exhaust plume and thermocouple No. 3 exposure and the posttest surface recession, the salt was ejected in the exhaust plume at the correct time.

In figure 16 for the supersonic plug location, the data indicated that thermocouple No. 1 did not break but was exposed barely at tailoff. Posttest examination verified that the thermocouple wire was just barely exposed on the surface of the nozzle. Again, the salt was ejected very early (19 sec as compared to exposure of the corresponding thermocouple at 30 sec).

The two remaining salt capsules that were not ejected were cross-sectioned. Figure 17 shows this cross section for the one intact in the subsonic location of nozzle S/N 02. In both cases the Grafoil was intact and below the final ablated surface by 0.005 to 0.015 in. These intact capsules indicate that adequate thermal protection was provided by the Grafoil for these particular capsules. This made the results from one capsule performance to the next extremely confusing and contradictory.

The test data were analyzed further to define the thermal adequacy of the Grafoil capsule by comparing the thermal penetration into the capsule with that recorded by the thermocouple plug. A comparison of these data for nozzle S/Ns 01 and 02 at both subsonic and supersonic locations is presented in figures 18 through 22.

As shown in figures 19 and 22, Grafoil provides an initial thermal lag for approximately the first 15 sec at which time the temperature recorded on the inner surface of the Grafoil capsule becomes essentially the same as that of the thermocouple plug. Late in the firing the capsule temperature decreased, indicating some effect of salt melting or other phase change, which caused absorption of energy. These results indicate that the actual capsule configuration used in this program was not adequate to reliably provide the sufficient thermal protection at elevated temperatures to prevent salt vaporization.

An exception to these results is shown in figure 20, which indicates that significant thermal protection was obtained throughout the firing. Once again, these results demonstrate the inconsistency of the encapsulation system performance which does not allow firm conclusions to be drawn.

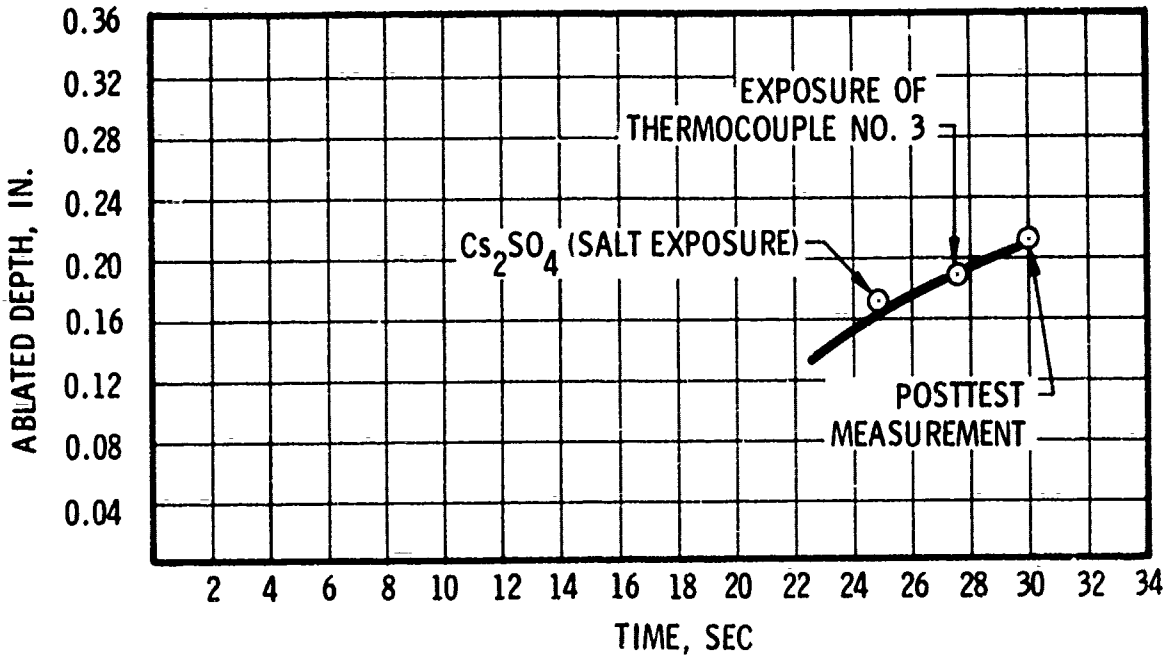

Figure 15. Surface Recession at Subsonic Thermocouple Plug Location, Silica-Phenolic Nozzle S/N 02

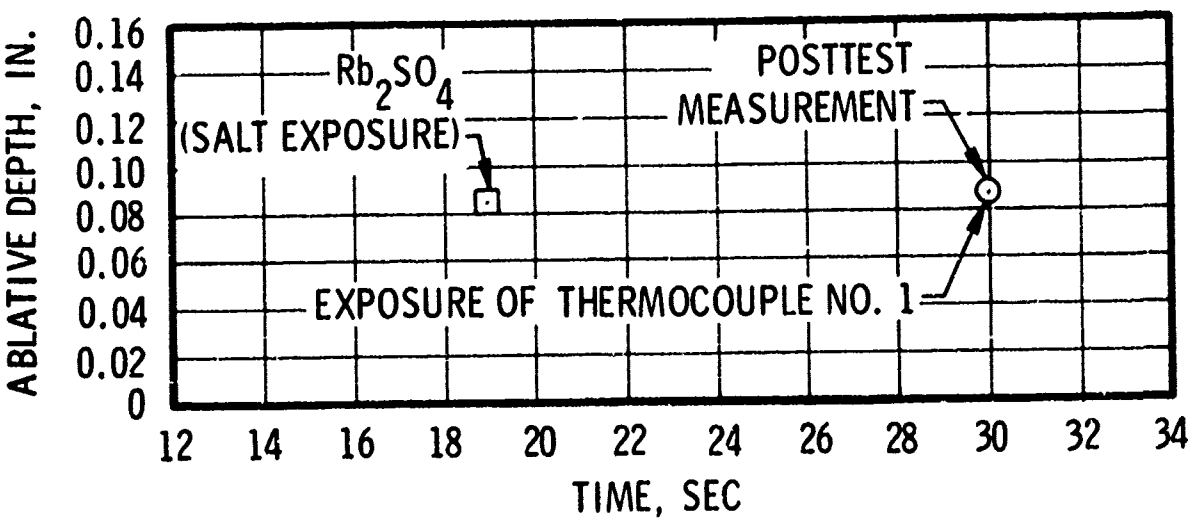

Figure 16. Surface Recession at Supersonic Thermocouple Plug Location, Silica-Phenolic Nozzle S/N 02

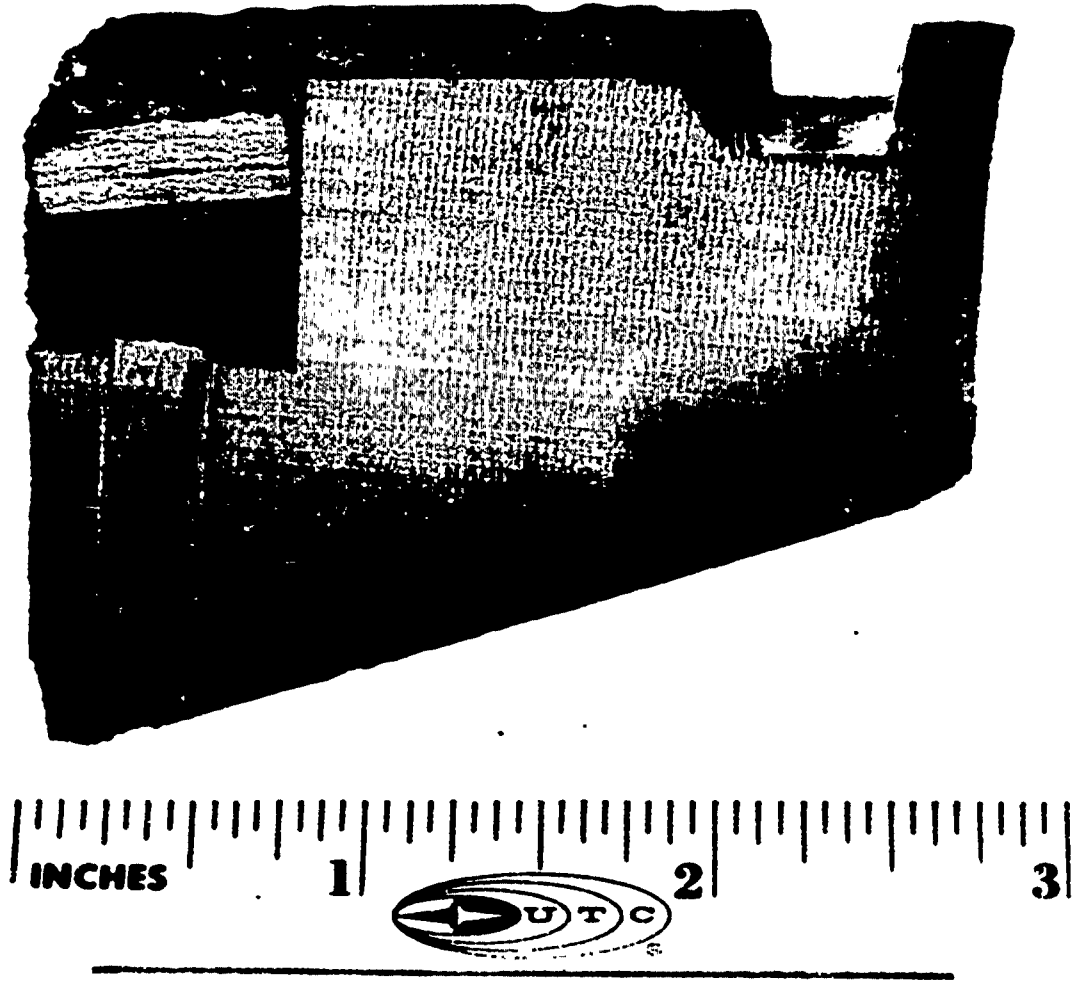

Figure 17. Cross Section of a Subsonic Salt Capsule

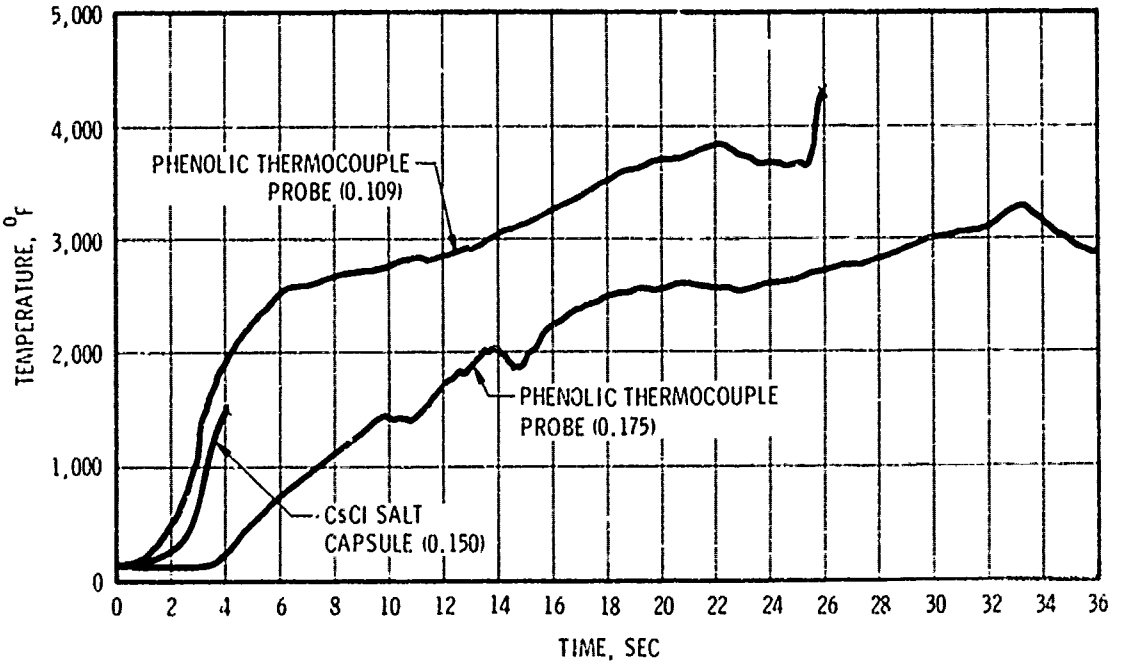

Figure 18. Comparison of the Recorded Temperature in the Tracer Capsule and Thermocouple Plug for Nozzle S/N 01 in the Subsonic Location

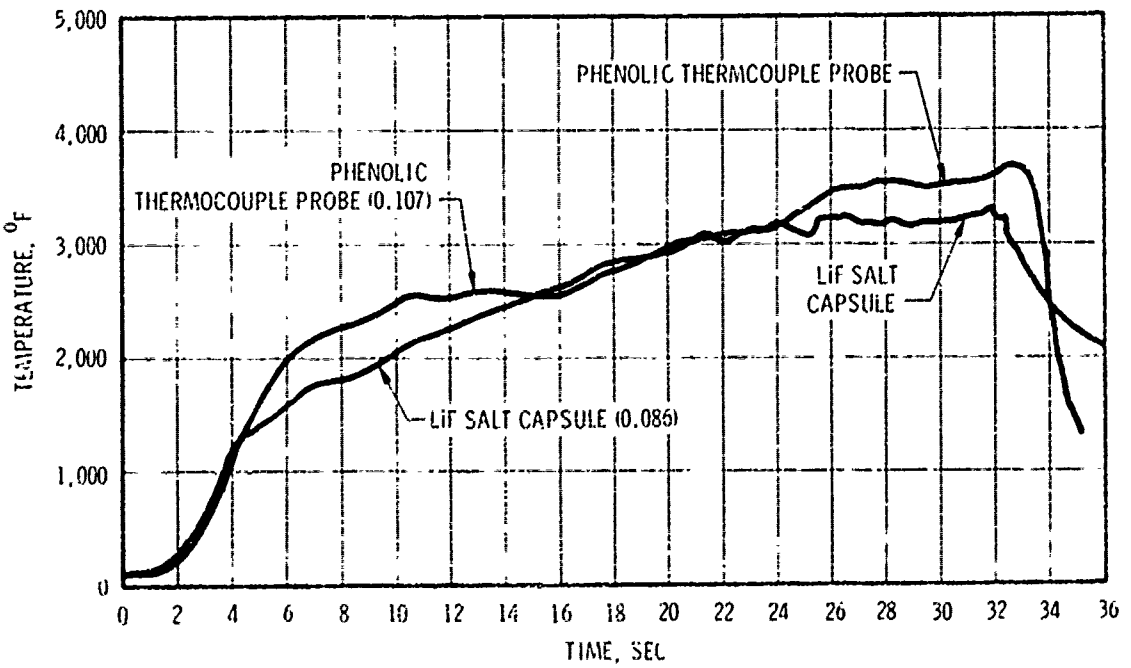

Figure 19. Comparison of the Recorded Temperature in the Tracer Capsule and Thermocouple Plug for Nozzle S/N 01 in the Supersonic Location (Lithium Fluoride Salt Capsule)

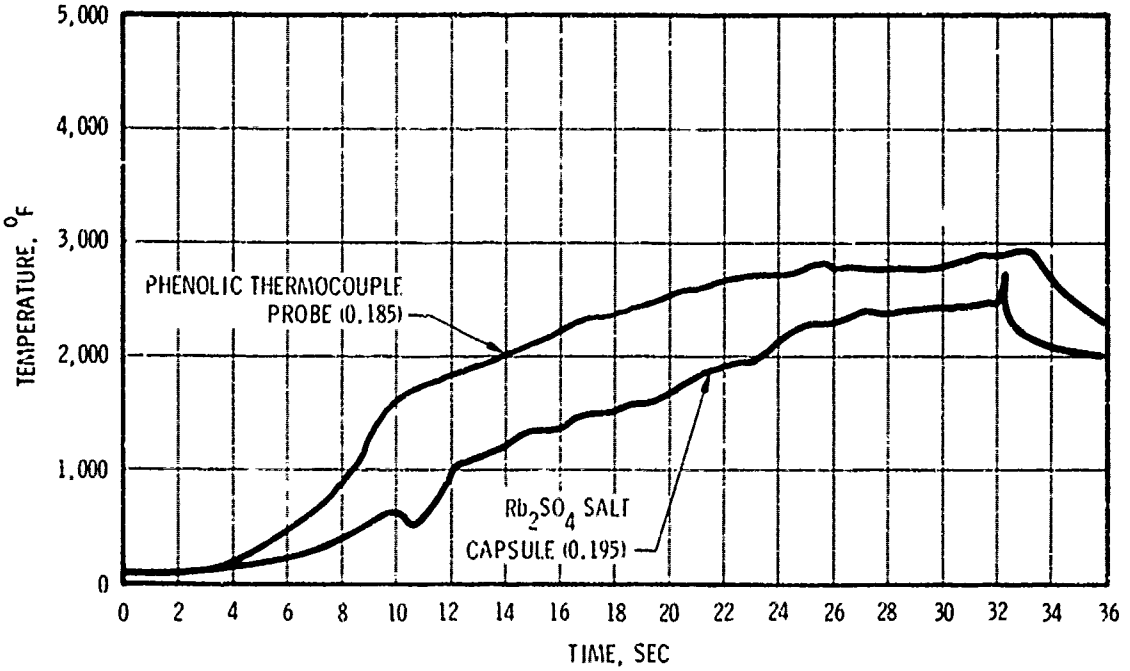

Figure 20. Comparison of the Recorded Temperature in the Tracer Capsule and Thermocouple Plug for Nozzle S/N 01 at the Supersonic Location (Rubidium Sulfate Salt Capsule)

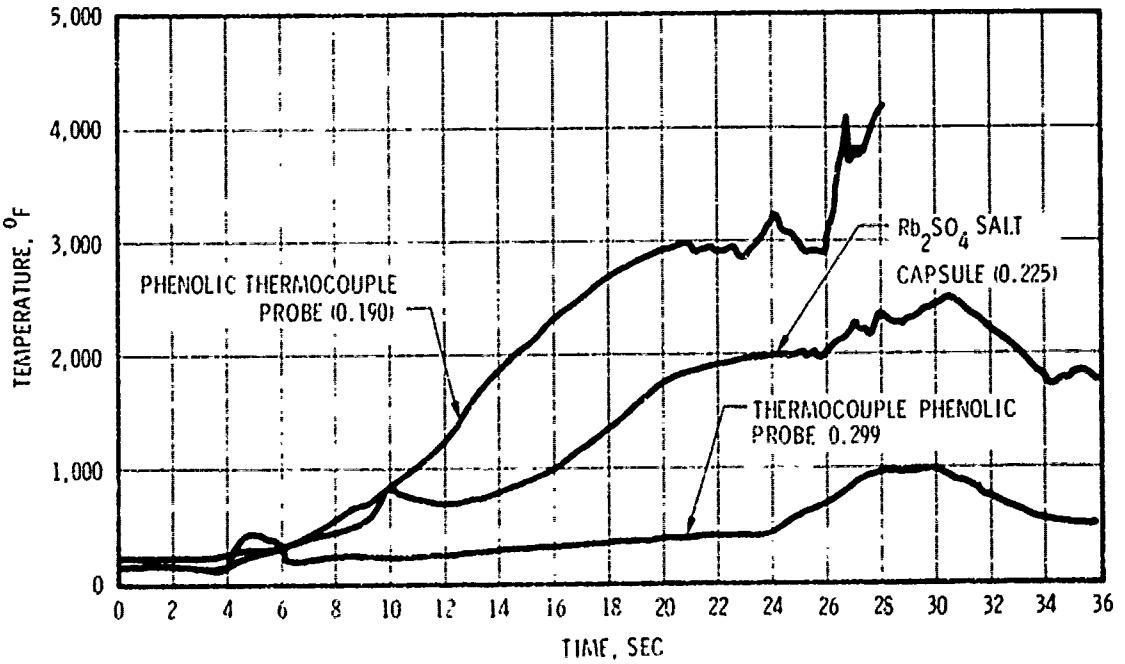

Figure 21. Comparison of the Recorded Temperature in the Tracer Capsule and Thermocouple Plug for Nozzle S/N 02 at the Subsonic Location

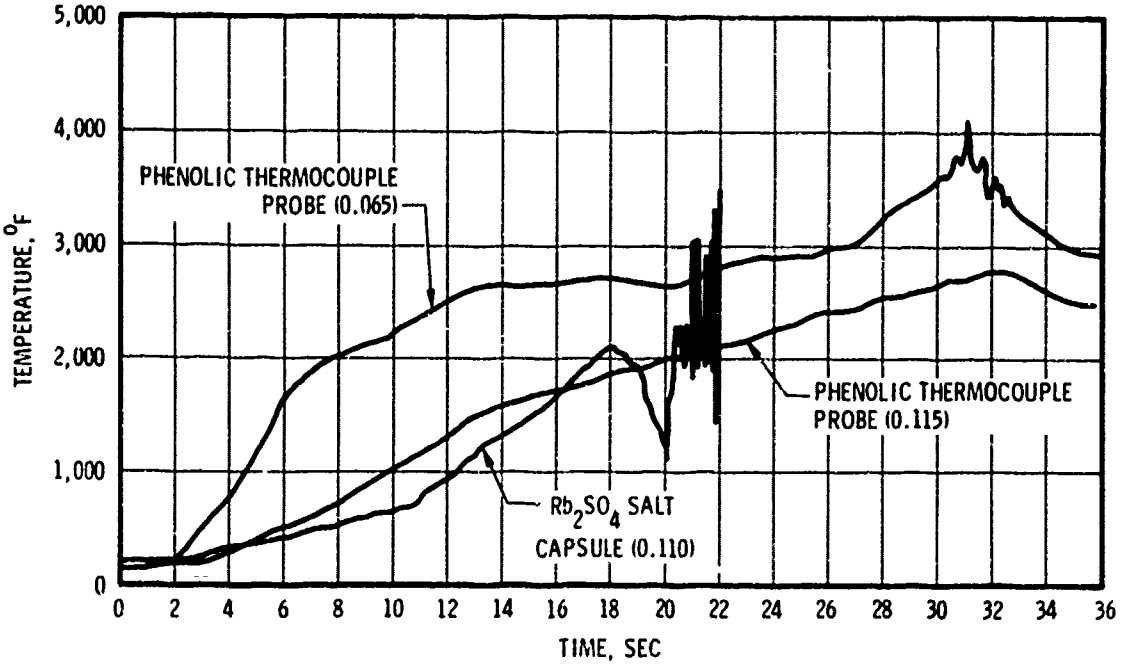

Figure 22. Comparison of the Recorded Temperature for the Tracer Capsule and Thermocouple Plug for Nozzle S/N 02 at the Supersonic Location

SECTION VIII

MAINTAINABILITY AND RELIABILITY

The full-scale test firings have demonstrated that the proposed encapsulation technique is highly unreliable with respect to the time of injection of the tracer salts into the exhaust stream. One of the capsules on nozzle S/N 02 ejected the tracers at the time of prediction whereas the other two capsules that were exposed on nozzle S/Ns 01 and 02 ejected the tracers considerably earlier than the time when the surface receded to the capsule location.

The proposed nozzle system containing instrumentation has no moving parts, and the capsules are all sealed; therefore, no maintainability is required.

SECTION IX

CONCLUSIONS

The conclusions drawn from the work conducted during this program are as follows:

A. The proposed Grafoil capsule configuration does not provide sufficient thermal penetration to allow demonstration of the accuracy of using tracer salts to measure in-situ ablation of ablating phenolic materials in actual rocket motor firings.

B. The tracer salts are detected immediately upon injection into the exhaust plume using spectrographic techniques.

C. The thermocouple plug is not an accurate method for verifying the accuracy of the tracer salt in-situ ablation method. This is due to uneven circumferential erosion effects and the high possibility of losing continuity on one or two thermocouples during the firing.

D. Use of a thermocouple inside the tracer capsule is very desirable for both laboratory and full-scale motor firings.

SECTION X

RECOMMENDATIONS

Recommendations are as follows:

A. The in-situ ablation measurement of nozzle ablative material using tracer salts does not show sufficient promise to warrant additional effort unless a considerably larger effort than that which was conducted on this program is undertaken.

B. Provided additional funds are allocated, the major area of activity should be in reevaluating the method of encapsulation to provide more thermal protection. The use of a molded (i.e., no bonded joints) capsule molded of thicker Grafoil is recommended.

APPENDIX

TRACER SIZING CRITERIA

The most important factor in the spectroscopic measurement is the quantity of the tracer element required to obtain a satisfactory signal. The smaller this quantity is, the easier the method will be to apply, but the spectral line must be strong enough to be clearly discernible above the continuum radiation. An analysis of the radiative properties of the exhaust plume is developed below.

The spectral radiance from a combination particle-gas cloud in a wavelength region where a spectral line is emitting is given by

$$N_\lambda(\lambda,T) = N^o_\lambda(\lambda,T) \left\{ 1 - \exp \left[- N_p \gamma_p \ell - Zsf(|\lambda_o - \lambda|) \right] \right\} \qquad (1)$$

where:

$N_\lambda(\lambda,T)$ = spectral line radiance

$N^o_\lambda(\lambda,T)$ = spectral radiance of a black body at temperature, T, and wavelength, λ

N_p = number density of radiating solid or liquid particles

γ_p = particle absorption cross section

ℓ = optical path length through the cloud

$Z = kn\ell$ = optical density of emitting gas

n = number density of radiating atoms

k = constant

$sf(|\lambda_o - \lambda|)$ = shape factor which determines characteristics of a spectral line

λ_o = center wavelength of line.

The continuum radiance can be given by

$$N^c_\lambda = N^o_\lambda(\lambda,T) \left[1 - \exp (- N_p \gamma_p \ell) \right] = N^o_\lambda(\lambda,T)\ \varepsilon_p\ (\lambda,T) \qquad (2)$$

where $\varepsilon_p(\lambda,T)$ is called the particle emissivity. From equations 1 and 2, the radiation of the line above the continuum radiation can be shown to be

$$N_\lambda^\ell(\lambda,T) = N_\lambda - N_\lambda^c - (N_\lambda^o - N_\lambda^c)\left[1 - \exp(-Zsf)\right] \quad (3)$$

The detection of the spectral line will depend on its relative intensity with respect to the continuum radiation; this will be a function not only of the line characteristics but also of the spectral bandpass of the filter or monochrometer used to make the measurement. The signal received at the detector as a result of the spectral line radiation can be represented as

$$E_\ell = 2K_1 \int_{\lambda_o}^{\lambda_o + \Delta\lambda^*} \tau(|\lambda_o - \lambda|)(N_\lambda^o - N_\lambda^c)\left[1 - \exp\left(-Zsf(|\lambda_o - \lambda|)\right)\right] d\lambda \quad (4)$$

and the continuum radiation signal as

$$E_c = 2K_1 \int_{\lambda_o}^{\lambda_o + \Delta\lambda^*} \tau(|\lambda_o - \lambda|)\, N_\lambda^c d_\lambda \quad (5)$$

where E_ℓ and E_c are signal voltages; K_1 is an apparatus constant; $\tau(|\lambda_o - \lambda|)$ represents the transmission characteristics of the filter or monochrometer; and $\Delta\lambda^*$ is the half width of the filter or monochrometer.

Assuming that N_λ^o and N_λ^c do not vary over the integration, the signal ratio can be written

$$E_\ell/E_c = \frac{N_\lambda^o - N_\lambda^c}{N_\lambda^c} \cdot \frac{\int_{\lambda_o}^{\lambda_o + \Delta\lambda^*} \tau\left[1 - \exp(-Zsf)\right] d\lambda}{\int_{\lambda_o}^{\lambda_o + \Delta\lambda^*} \tau d\lambda} \quad (6)$$

This relationship indicates that the transmission characteristics of the filter or monochrometer as well as the shape of the spectral line are important in determining the signal ratio obtained.

The significance of this relationship will become clear from an evaluation of these integrals under various conditions, using sodium as the trace element. The following assumptions are made:

A. $\tau(|\lambda_o - \lambda|)$ is a step function such that

$$\tau = 0 \text{ for } |\lambda_o - \lambda| > \Delta\lambda^*$$
$$\tau = 1 \text{ for } |\lambda_o - \lambda| \leq \Delta\lambda^*$$

B. The continuum emissivity $\varepsilon_p = 0.5$. This is based on data from exhaust plumes of rocket motors containing 16% aluminum in a hydrocarbon binder and ammonium perchlorate. According to measurements made at UTC, this value does not vary appreciably for the plumes of motors ranging in thrust from 1,000 to over 1,000,000 lb. For smaller motors the data indicate that ε_p decreases, which would result in a higher E_ℓ/E_c signal to continuum ratio or allow a reduction in the quantity of seed required to obtain the same E_ℓ/E_c signal.

With these assumptions

$$E_\ell/E_c = \frac{N_\lambda^o (1 - \varepsilon p) \int_{\lambda_o}^{\lambda_o + \Delta\lambda^*} \tau \left[1 - \exp(-Zsf)\right] d\lambda}{N_\lambda^o \varepsilon p \int_{\lambda_o}^{\lambda_o + \Delta\lambda^*} \tau \, d\lambda} \tag{7}$$

or

$$E_\ell/E_c = \frac{\int_{\lambda_o}^{\lambda_o + \Delta\lambda^*} \left[1 - \exp(-Zsf)\right] d\lambda}{\Delta\lambda^*} \tag{8}$$

The shape factor sf for collision-broadened line shapes may be expressed as

$$sf = \frac{b^2}{b^2 + (\lambda_o - \lambda)^2} \tag{9}$$

where b is the collision half width. Bundy* indicates that for sodium at atmospheric pressure and 2,200°K, b is 0.04 Å and the optical depth Z is $1.5 \times 10^{-13} n\ell$, where n is the number density of sodium atoms and ℓ the path length through the plume.

*Bundy, Strong, and Gregg, Journal of Applied Physics, Vol. 22, No. 8, August 1951.

Using these values, equation 8 was evaluated for several optical depths Z and several filter transmission bandwidths $\Delta\lambda^*$. The results are shown in figure 23 which plots the ratio E_ℓ/E_c as a function of Z with $\Delta\lambda^*$ as the parameter. This plot shows the signal ratio which will be obtained with a particular bandpass filter as a function of the optical depth, and thus makes it possible to calculate the amount of sodium required to obtain a particular signal ratio.

The rate at which sodium must be added to the rocket motor exhaust plume to produce the desired optical depth is

$$\dot{m}_{Na} = \frac{\dot{m}_T M_{Na} n}{\rho_B N_o} \tag{10}$$

where M_{Na} is the molecular weight, $\dot{m}_T$ the rocket mass flow rate, ρ_B the rocket gas density, and N_o is Avagadro's number.

With

$$n = \frac{Z}{1.5 \times 10^{13} \ell} = 0.667 \times 10^{13} \frac{Z}{\ell} \tag{11}$$

and using NaCl as the practical form for the introduction of sodium, the addition rate is

$$\dot{m}_{NaCl} = 6.48 \times 10^{-10} \frac{\dot{m}_T Z}{\rho_B \ell} \tag{12}$$

For a large solid rocket motor using the described propellant, with a mass flow rate $m_T = 2.5 \times 10^6$ g/sec, a gas density, $\rho_B = 1.32 \times 10^{-4}$ g/cm^3, and a plasma path length $\ell = 2.9 \times 10^2$ cm, and noting from figure 23 that for a signal/continuum ratio $E_\ell/E_c = 0.5$ the optical depth must be $Z = 3.2 \times 10^2$, a salt addition rate $\dot{m}_{NaCl}$ of 13.6 g/sec (approximately 6.7 cc/sec) is obtained.

The actual amount of salt that must be inserted at each point will depend upon the length of time that is needed to observe and record the signal. Experience indicates that this time is approximately 100 msec or less, therefore, 1.36 g or 0.67 cc are needed.

The mass flow rate of a rocket motor varies directly as the thrust, F, and the distance through the plume, ℓ, varies as the square root of F. Thus, the quantity of the tracer element that must be added to rocket motors using the same propellant but with different thrust levels varies with the square root of the thrust. This is shown in figure 24 for a signal ratio level of 0.5, using various bandwidth filters. It is evident that a decrease in the bandpass of the filter or monochrometer greatly reduces the amount of salt required to give a satisfactory signal ratio.